

LIBRARY
ROYAL AIRCRAFT ESTABLISHMENT
BEDFORD.

C.P. No. 1178

C.P. No. 1178



MINISTRY OF DEFENCE (AVIATION SUPPLY)

AERONAUTICAL RESEARCH COUNCIL

CURRENT PAPERS

Theoretical Pressure Distributions
on Four Simple Wing Shapes
for a Range of Supersonic
Flow Conditions

by

J. Pike

Aerodynamics Dept., R.A.E., Bedford

LONDON: HER MAJESTY'S STATIONERY OFFICE

1971

PRICE 70 p NET

C.P. No.1178*

March 1971

LIBRARY
ROYAL AIRCRAFT ESTABLISHMENT
BEDFORD.

THEORETICAL PRESSURE DISTRIBUTIONS ON FOUR SIMPLE WING SHAPES FOR
A RANGE OF SUPERSONIC FLOW CONDITIONS

by

J. Pike

SUMMARY

Pressure distributions are presented for four conical wing shapes with attached shock waves at their leading edges. The wings are those proposed after Euromech 20 as reference shapes for the comparison of flow prediction methods. The influence on the pressure distribution of wing incidence, free stream Mach number or ratio of specific heats is demonstrated. Some pressure distributions over the upper surface are also presented, assuming an isentropic expansion at the leading edge.

* Replaces RAE Technical Report 71064 - ARC 33040

CONTENTS

| | <u>Page</u> |
|------------------------------|--------------|
| 1 INTRODUCTION | 3 |
| 2 THE PRESSURE DISTRIBUTIONS | 4 |
| Tables 1-4 | 6 |
| References | 9 |
| Illustrations | Figures 1-39 |
| Detachable abstract cards | - |

1 INTRODUCTION

Following Euromech 20¹ Roe has proposed two caret and two plane delta wings² to be used to compare results from various methods for predicting the flow about such wings. In this Report the method of Ref.3 has been used to predict the flow over these wings. This method is only applicable to wings with attached shock waves. It uses a small perturbation technique behind a plane shock wave combined with an empirical modification which tends to reduce the second order errors. The results when compared with known flow conditions³ show good agreement, except for flows with very large pressure changes in the internal flow. Some comparisons with 'exact' numerical calculations are also shown here (Figs.27-29).

The wing and flow conditions suggested by Roe are shown here in Figs.1-7 reproduced from Ref.2. Fig.1 gives the details of the wings, Fig.2 shows how certain flow regions are labelled. Line PQR represents shock wave detachment, and line SQT the conditions for a plane shock wave. Figs.3-7 show the flow conditions selected and their relation to the regions of Fig.2. The numbers form part of a general labelling system, used to label Figs.8-39, of the form:-

letter A to D denoting the wing as in Fig.1;

digit 0-9 denoting Mach number according to the code 0 for 2.6, 1 for 3, 2 for 3.5, 3 for 4, 4 for 4.5, 5 for 5, 6 for 6, 7 for 7.5, 8 for 8, 9 for 10;

digit 1-5 in order of ascending angle of incidence;

letter U or L denoting the flow over the upper or lower surfaces, respectively;

below this label, the values of the flow variables γ , M and α are indicated, as also is the flow regime (A, B, C or D) according to the classification of Fig.2.

For example, the plot in Fig.27 is labelled D31L, with 1.4, 4, 5, B below. This denotes the lower surface of the delta wing with the leading edge having a sweep angle of 50° at flow condition 31 (see Fig.7). Flow condition 31 means $M_\infty = 4$ and $\alpha = 5$, as is shown in Fig.7. Also included in the table is the information that $\gamma = 1.4$ and the flow regime is of type B (see Fig.2).

2 THE PRESSURE DISTRIBUTIONS

Near the lines PU and SQ of Fig.2, the pressure distribution can be obtained³ by linearising about either the free stream or the parallel flow behind a plane shock wave. A simple semi-empirical formula has been developed³ which includes both of these cases in a single expression. This expression has been shown to give good estimates of the pressure distributions over the whole of regions A and B except near the boundary line PQT. It has also been applied to the upper surfaces, although it is only theoretically justifiable for small upper surface incidence.

Figs.8-10 each show the pressure distribution for a wing over a range of incidence at the same Mach number. Fig.8 shows wing A at $M = 10$. Fig.9 shows wing B for $M = 5$, Fig.10 shows wing D at $M = 4$. Both upper and lower surface pressure distributions are shown for $\gamma = 1.4$ and 1.25. It can be observed that changing γ makes very little difference to the pressure distribution at low incidence, but near detachment significant changes occur both in the pressure coefficients and the detachment conditions.

The results of a systematic investigation of all the conditions proposed by Roe are summarised in Tables 1-4 for wings A to D. Wing A has finite thickness, and for conditions 1, 12, 21, 42, 62 and 92 the upper surface is very nearly streamwise. For region D, all the leading edge shock waves were found to be detached including that of B33 (see Figs.4 and 5). The wing and flow conditions where the leading edge is subsonic are listed in Tables 1-4. For the conditions A41, the upper surface shock wave is detached, causing an otherwise attached lower surface shock wave to be detached also. It should be noted that the lower surface pressure distribution of Fig.11 does not allow for upper surface influence.

The lower surface pressure distributions for regions A and B are shown in Figs.11-29 with y/y_{\max} a spanwise coordinate normal to the ridge line. The C_p axis has a false zero to accentuate the pressure changes. The ratio of the C_p scale to the y/y_{\max} scale is given by the value of r , shown near the C_p axis. Each pressure distribution has been given a separate figure to facilitate the comparison with other estimates. Only limited comment is included here on the pressure distributions, a critical assessment being left until after the comparisons have been made.

The region of constant pressure coefficient near the leading edge is obtained from oblique shock wave theory⁴, and is exact over the conically

supersonic region of the wing for inviscid flow. For the flow conditions of region B, where an expansion occurs near the centre of the wing, the true position of the conical sonic point is indicated. For region A, the pressure rise shown may indicate the presence of a second shock wave and the conically sonic position can no longer be obtained from the exact leading-edge conditions. Near detachment in region B, the present theory predicts too large a region of constant pressure, as shown particularly in Fig.26. For most of regions A and B, away from the boundary line PQT the pressure distributions have been found to be surprisingly accurate³. Comparison with the results of Voskresenskii⁵ for plane deltas is shown in Figs.27-29. Unfortunately it is difficult to plot the results (taken from Ref.6) accurately on the expanded scale used. However the best estimate of them corresponds closely with the predicted pressures, except for the region of rapid pressure change in D33.

Figs.30-39 show a selection of upper surface pressure distributions, which tend to indicate that the variation in the pressure on the upper surface is much smaller than on the lower surfaces.

In Figs.8-39 the average pressure coefficient (\bar{C}_p) is indicated. The lift coefficient of the wing is of course the difference between \bar{C}_p on the upper surface, and \bar{C}_p on the lower surface. Also shown is the pressure coefficient on an unswept wedge at the same incidence and Mach number (C_{pw}).

The time to evaluate a pressure distribution using an ICL 4130 computer was about $\frac{1}{2}$ second to find C_{pe} and C_{pw} , plus $\frac{1}{20}$ second for each pressure value.

Table 1WING A, $\gamma = 1.4$

| | |
|-----|--|
| A1 | Subsonic leading edge |
| A11 | Shock wave detached |
| A12 | Subsonic leading edge |
| A21 | Shock wave detached |
| A41 | Fig.11 NB. Upper surface shock wave detached |
| A42 | Shock wave detached |
| A43 | Shock wave detached |
| A61 | Fig.12 |
| A62 | Fig.13 |
| A63 | Shock wave detached |
| A81 | Fig.14 |
| A82 | Fig.15 |
| A83 | Shock wave detached |
| A91 | Figs.8, 16 and 30 |
| A92 | Figs.8 and 17 |
| A93 | Figs.8, 18 and 31 |
| A94 | Figs.8 and 19 |
| A95 | Shock wave detached |

Table 2WING B, $\gamma = 1.4$

| | |
|-----|--------------------------------------|
| B11 | Shock wave detached |
| B12 | Shock wave detached |
| B13 | Shock wave detached |
| B31 | Fig.20 |
| B32 | Fig.21 |
| B33 | Shock wave detached |
| B34 | Shock wave detached |
| B51 | Figs.9, 22 and 32 |
| B52 | Figs.9, 23 and 33 |
| B53 | Thin wing leading edge subsonic |
| B54 | Thin wing leading edge subsonic |
| B55 | Shock wave detached |
| B71 | Figs.24 and 34 |
| B72 | Thin wing leading edge subsonic |
| B73 | Thin wing leading edge subsonic |
| B74 | Equivalent wedge shock wave detached |

Table 3WING C, $\gamma = 1.4$

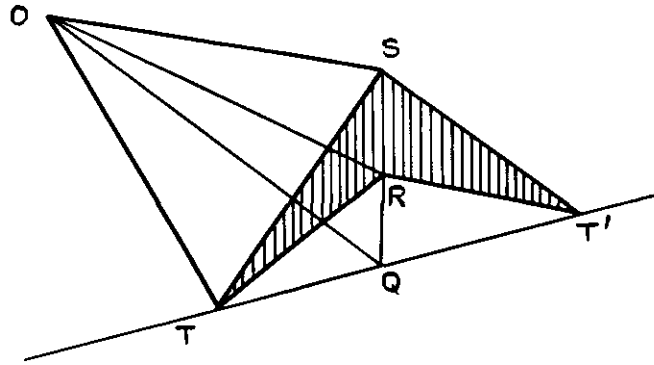
| | |
|-----|-----------------------|
| C11 | Subsonic leading edge |
| C12 | Subsonic leading edge |
| C13 | Shock wave detached |
| C41 | Shock wave detached |
| C42 | Shock wave detached |
| C43 | Shock wave detached |
| C91 | Figs.25 and 35 |
| C92 | Figs.26 and 36 |
| C93 | Shock wave detached |
| C94 | Shock wave detached |

Table 4WING D, $\gamma = 1.4$

| | |
|-----|--------------------|
| D31 | Figs.10, 27 and 37 |
| D32 | Figs.10, 28 and 38 |
| D33 | Figs.10, 29 and 39 |

REFERENCES

| <u>No.</u> | <u>Author(s)</u> | <u>Title, etc.</u> |
|------------|--------------------------------------|--|
| 1 | P.L. Roe L. Davies L.C. Squire | Report on Euromech 20. RAE Technical Report 71054 (1971) |
| 2 | P.L. Roe | Unpublished RAE Memorandum |
| 3 | J. Pike | The flow past flat and anhedral delta wings with attached shock waves. Unpublished RAE Report |
| 4 | J. Pike | Attached flow conditions on sharp supersonic leading edges. Unpublished RAE Report |
| 5 | G.P. Voskresenskii | Numerical solution of the problem of a supersonic gas flow past an arbitrary surface of a delta wing in the compression region. Izv. Akad. Nauk. SSSR, Mekh. Zhid. 1. Gaza, 4 (1968) |
| 6 | J.C. South, Jnr. E.B. Klunker | Methods for calculating non-linear conical flows. NASA SP 228 (1969) |

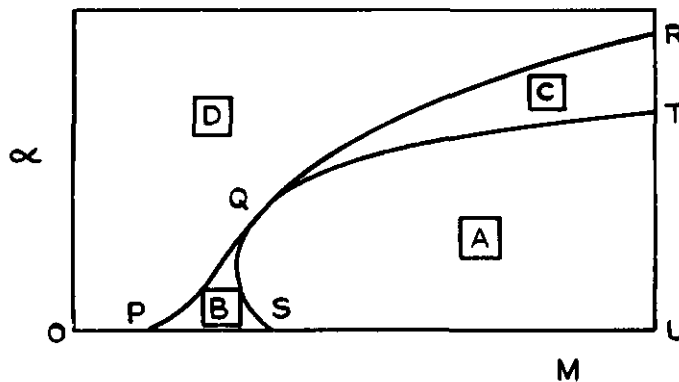


| | QOR | ROS | OTQ | TRT' |
|---|-------|------|-------|--------|
| A | 6.51 | 7.49 | 73.77 | 137.44 |
| B | 12.00 | 0 | 75.00 | 104.38 |
| C | 0 | 0 | 75.00 | 180.00 |
| D | 0 | 0 | 50.00 | 180.00 |

Notes

- 1 Wing A has a 'relastic' thickness. The others are assumed ideally thin
- 2 The values quoted for angle TRT' is the true angle between the facets ORT, ORT', ie it is measured normal to the line OR

Fig.1 Angles defining the standard wings



α is the incidence of the line OR

Fig2 Schematic (M, α) diagram

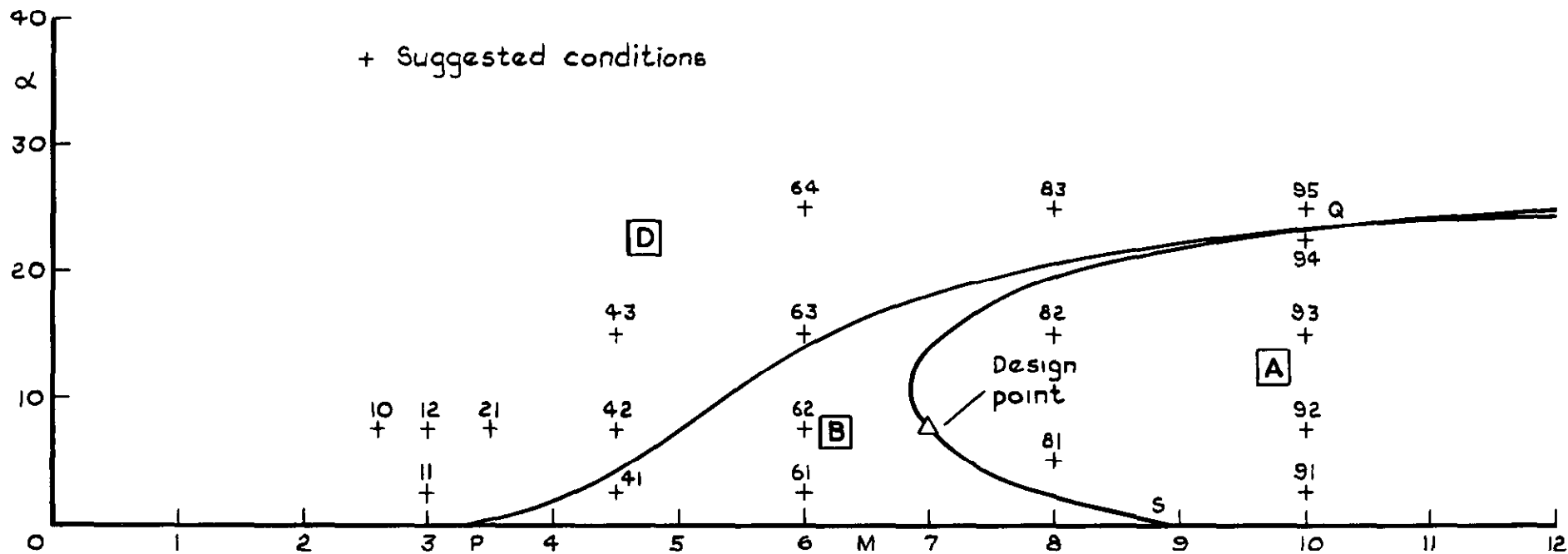


Fig.3 Wing A

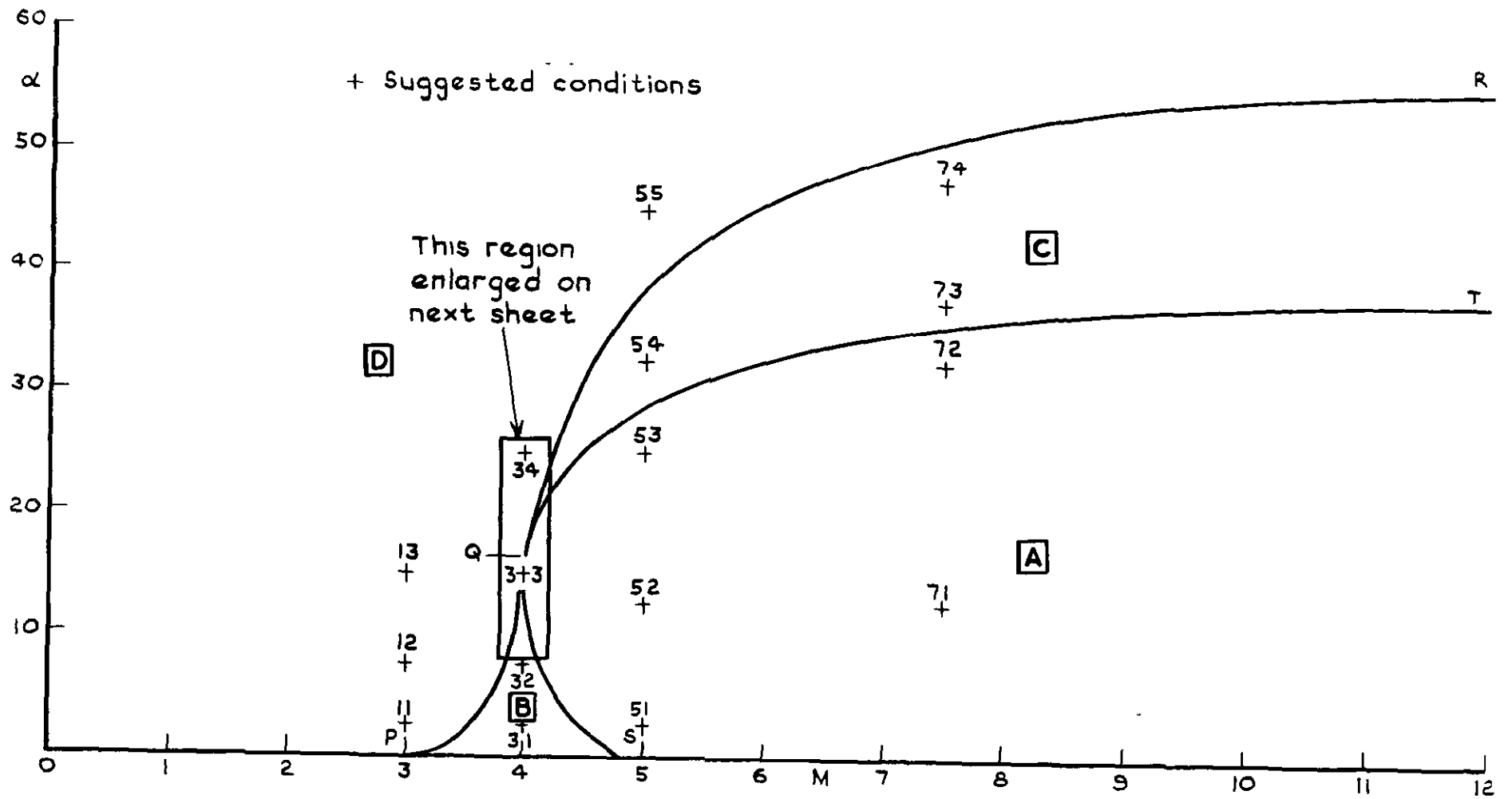


Fig.4 Wing B

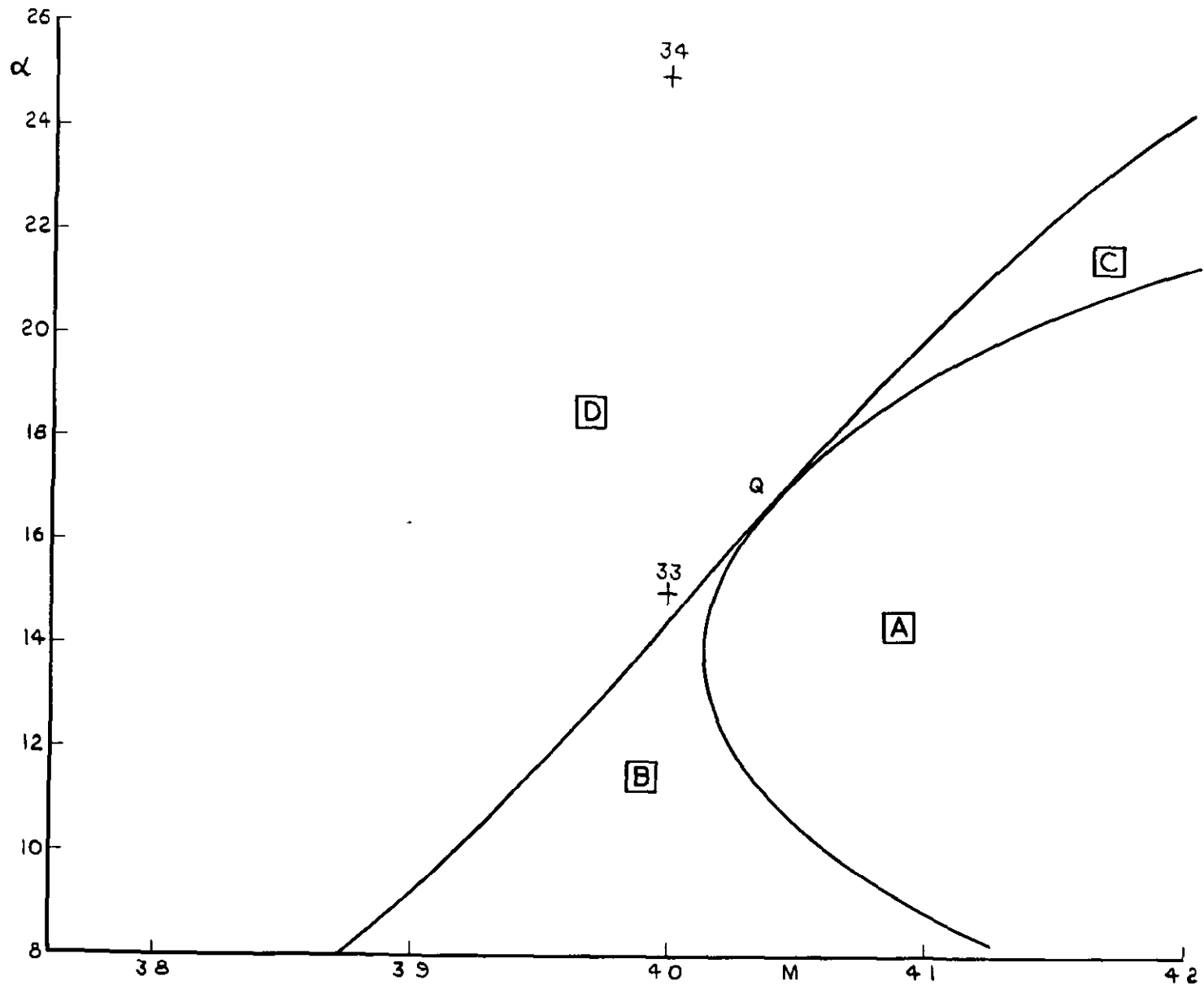


Fig.5 Wing B (enlargement)

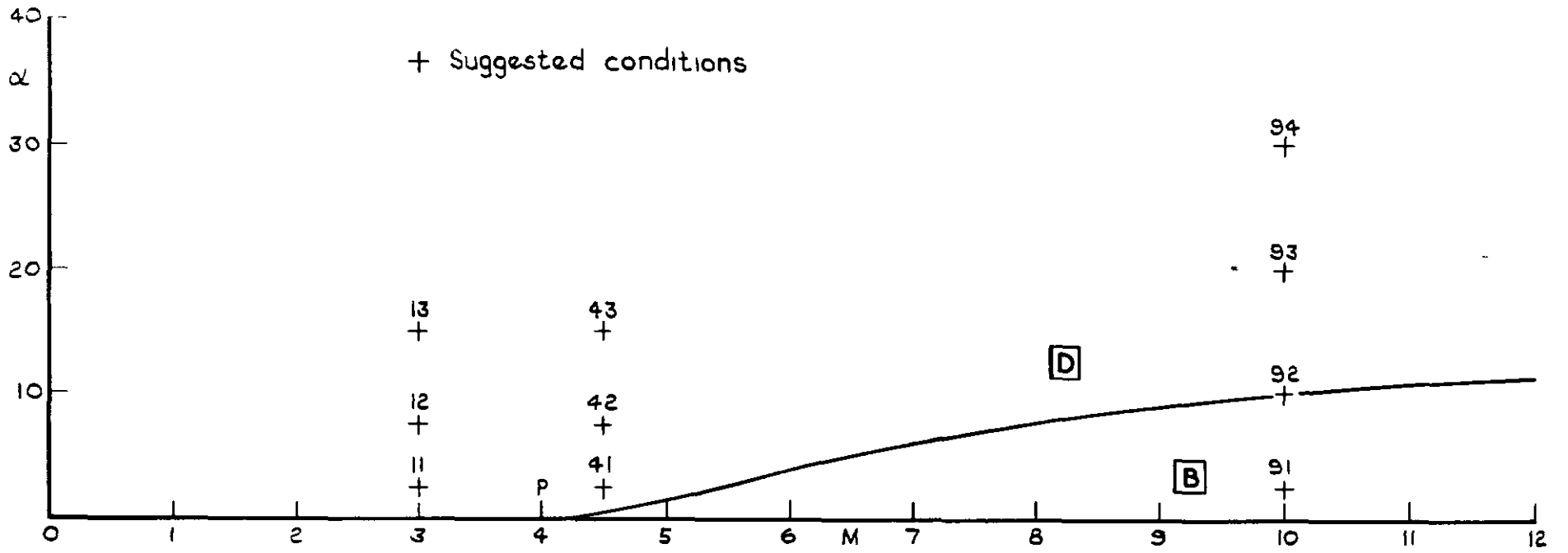


Fig 6 Wing C

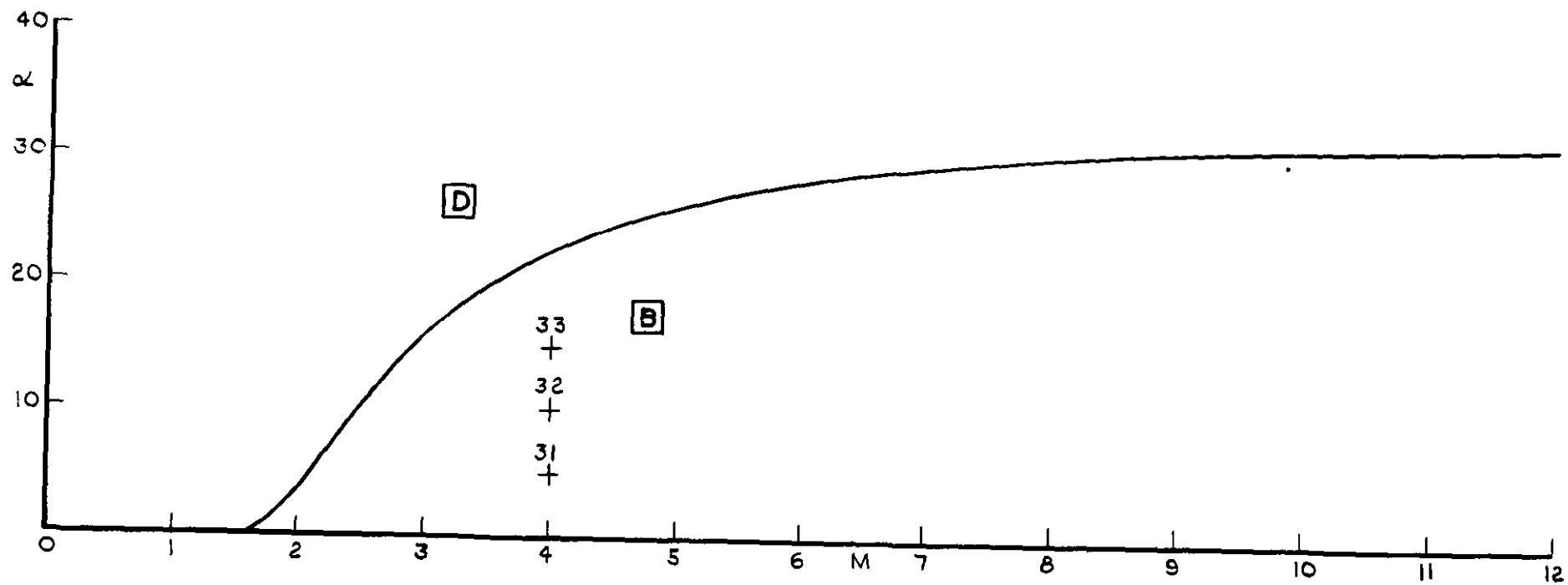


Fig. 7 Wing D

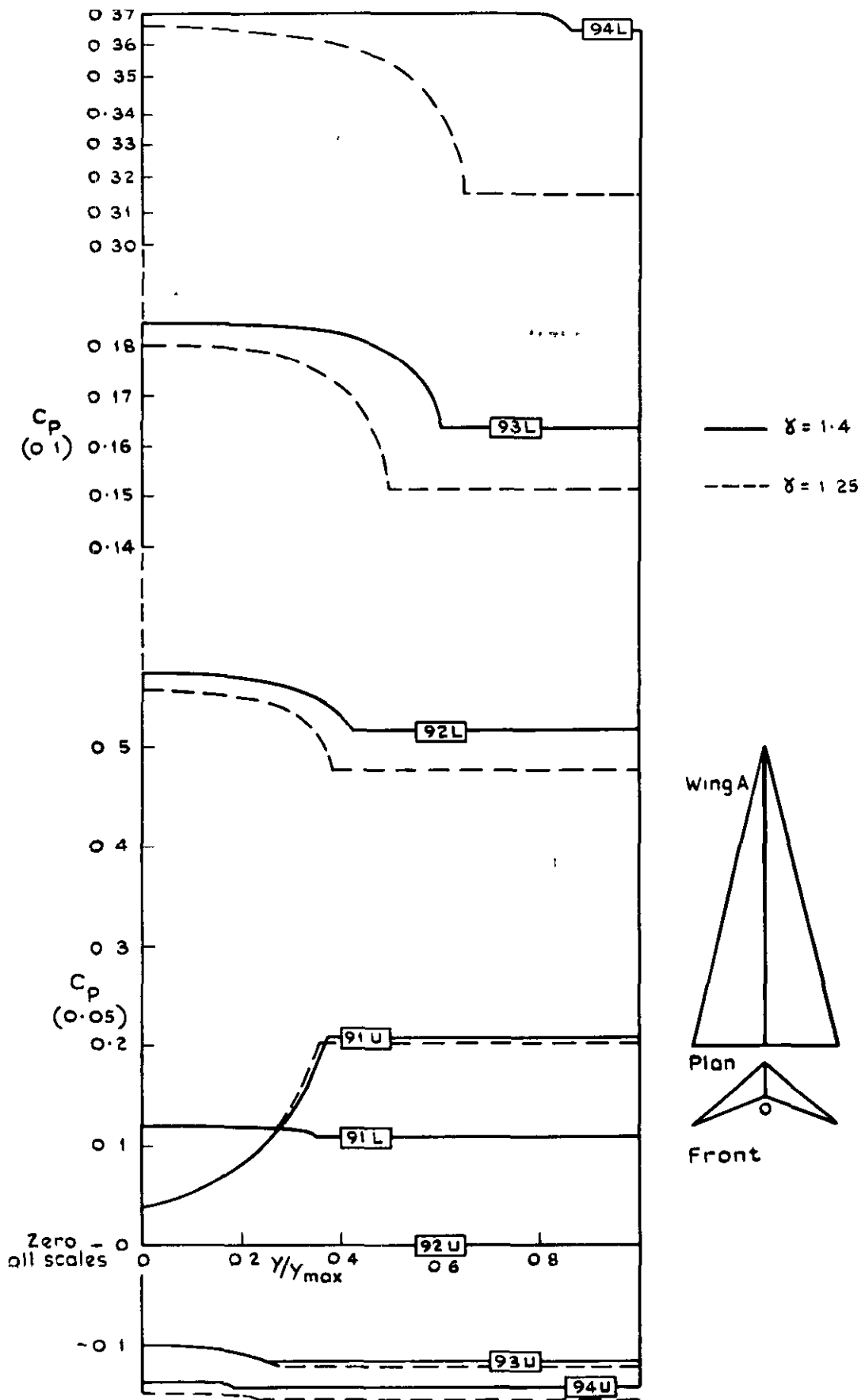


Fig.8 Wing A: Surface pressure coefficients on the upper and lower surfaces at $M=1.0$

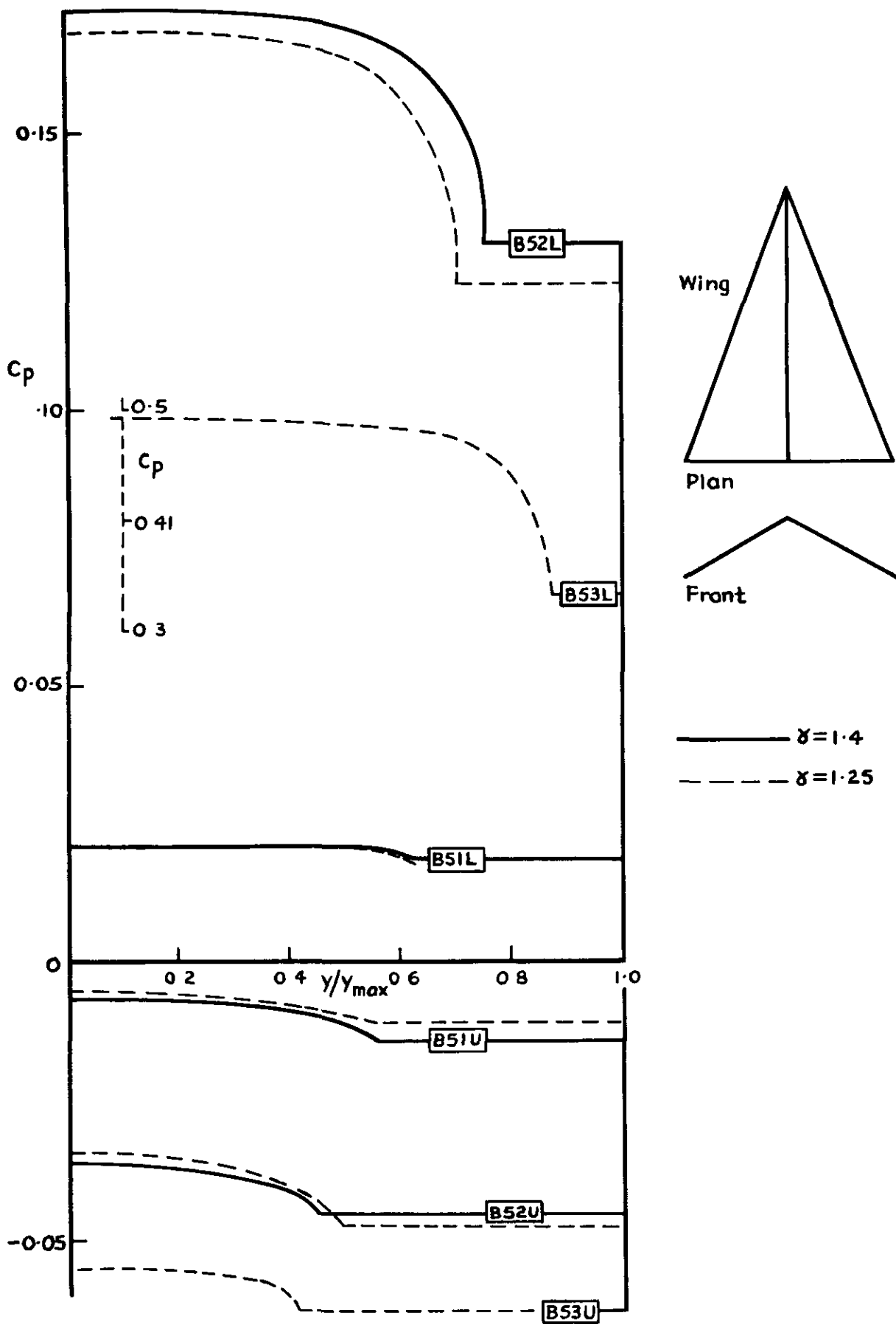


Fig.9 Wing B: Surface pressure coefficient on the upper and lower surfaces at $M=5$

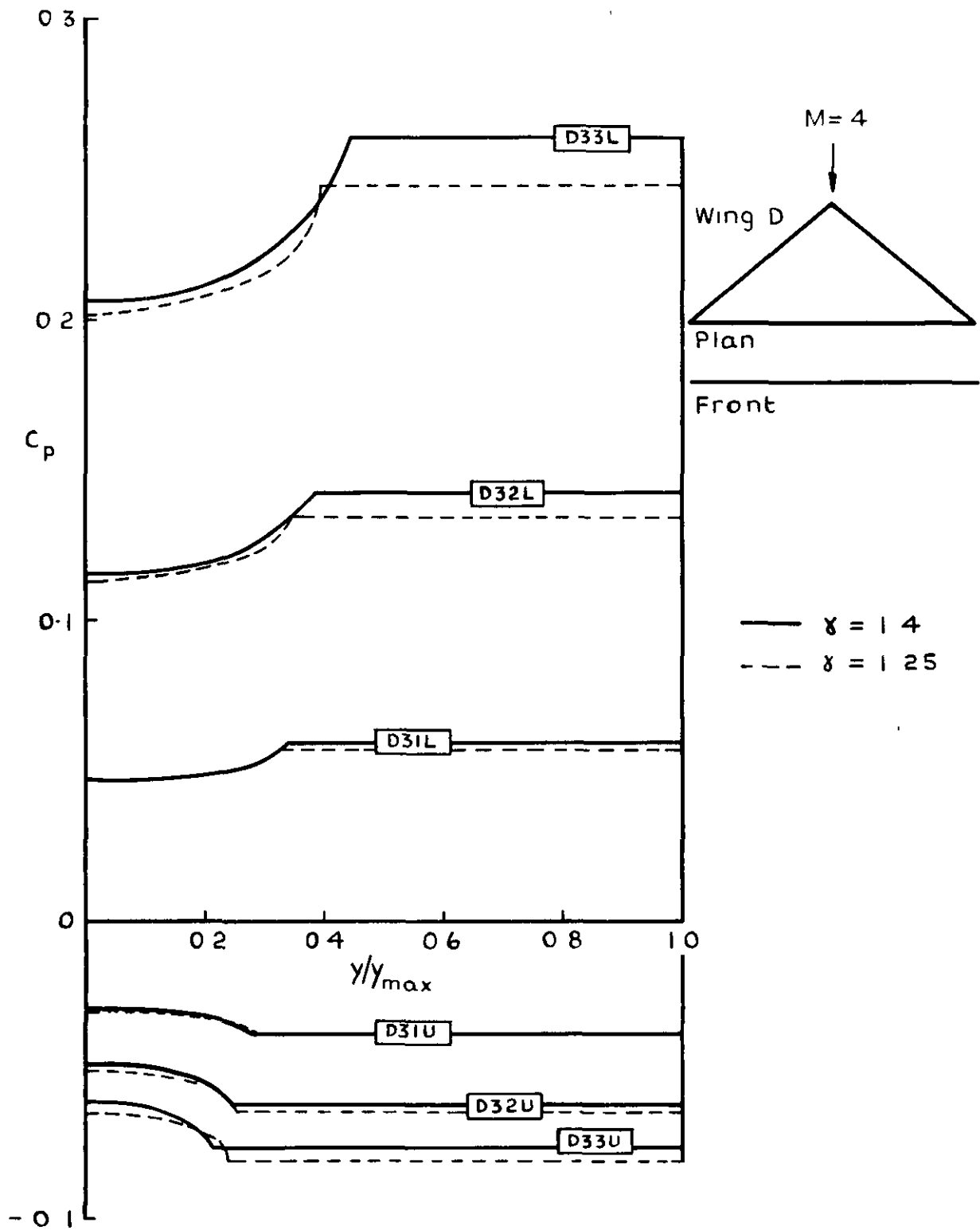


Fig.10 Wing D: Surface pressure coefficient on the upper and lower surfaces at $M = 4$

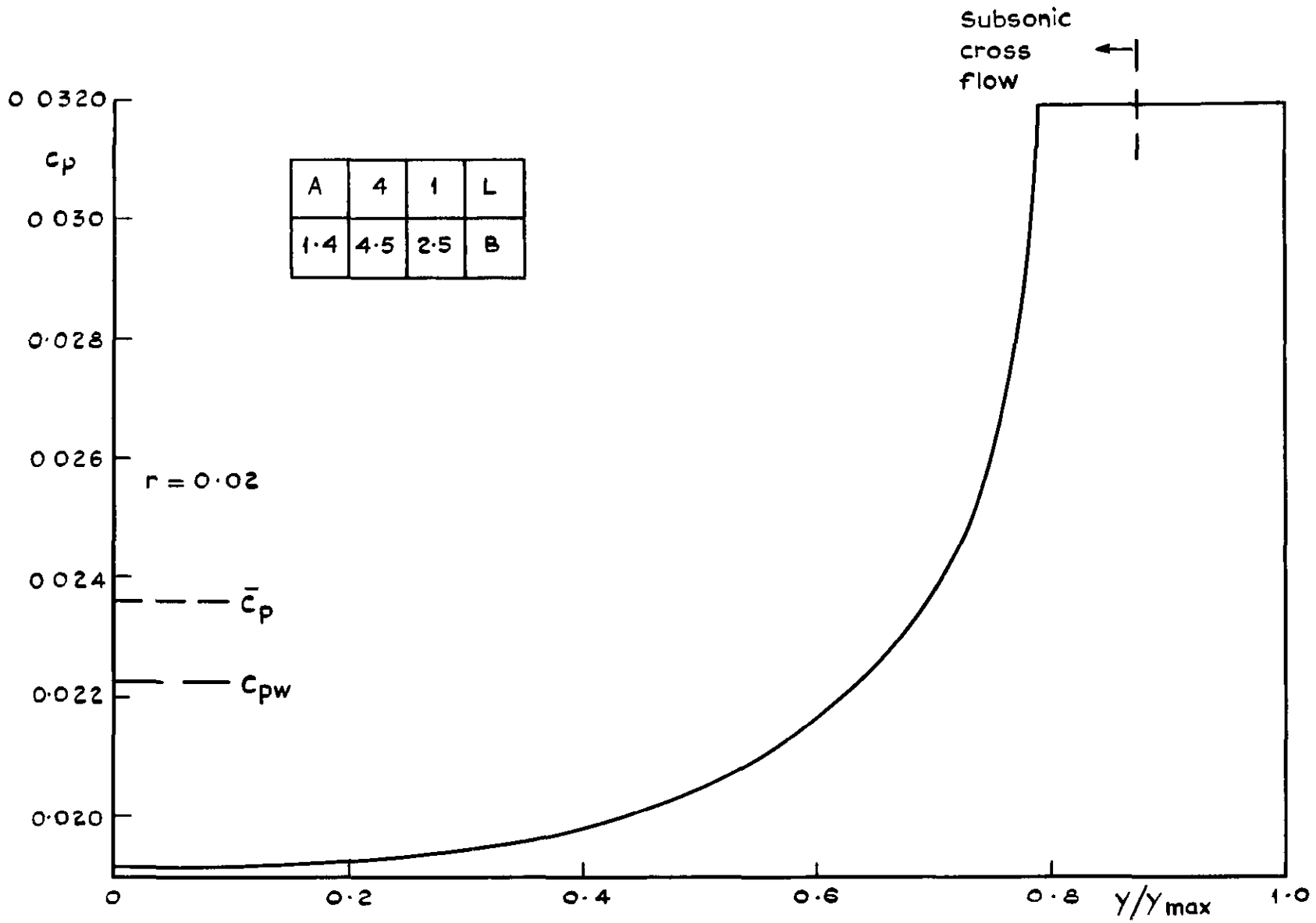


Fig. 11 Wing A: Pressure distribution across span $M = 4.5$, $\chi = 1.4$, $\alpha = 2.5^\circ$

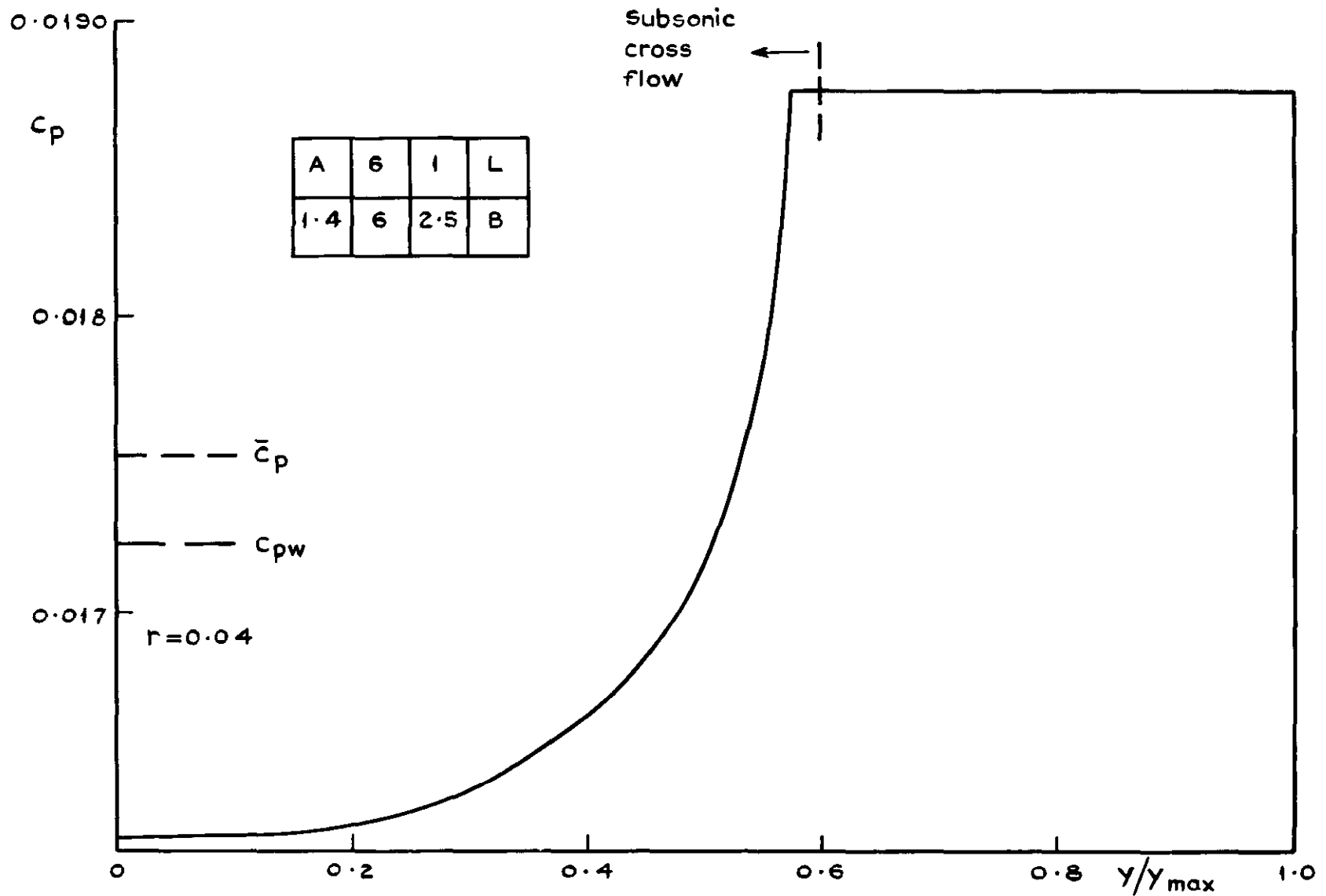


Fig. 12 Wing A: Pressure distribution across span $M=6$, $\delta=1.4$, $\alpha=2.5$

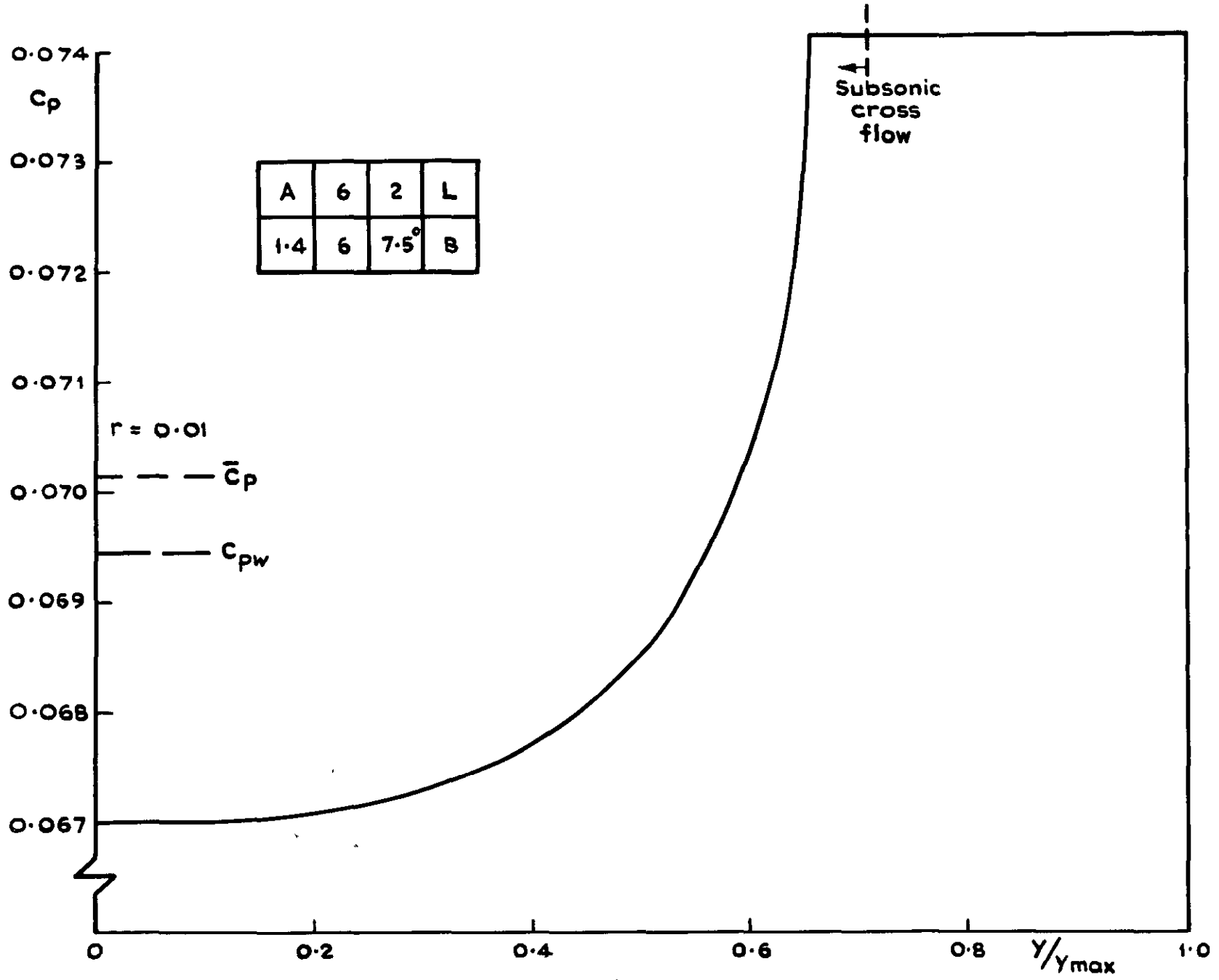


Fig.13 Wing A: Pressure distribution across span $M = 6$, $\gamma = 1.4$, $\alpha = 7.5^\circ$

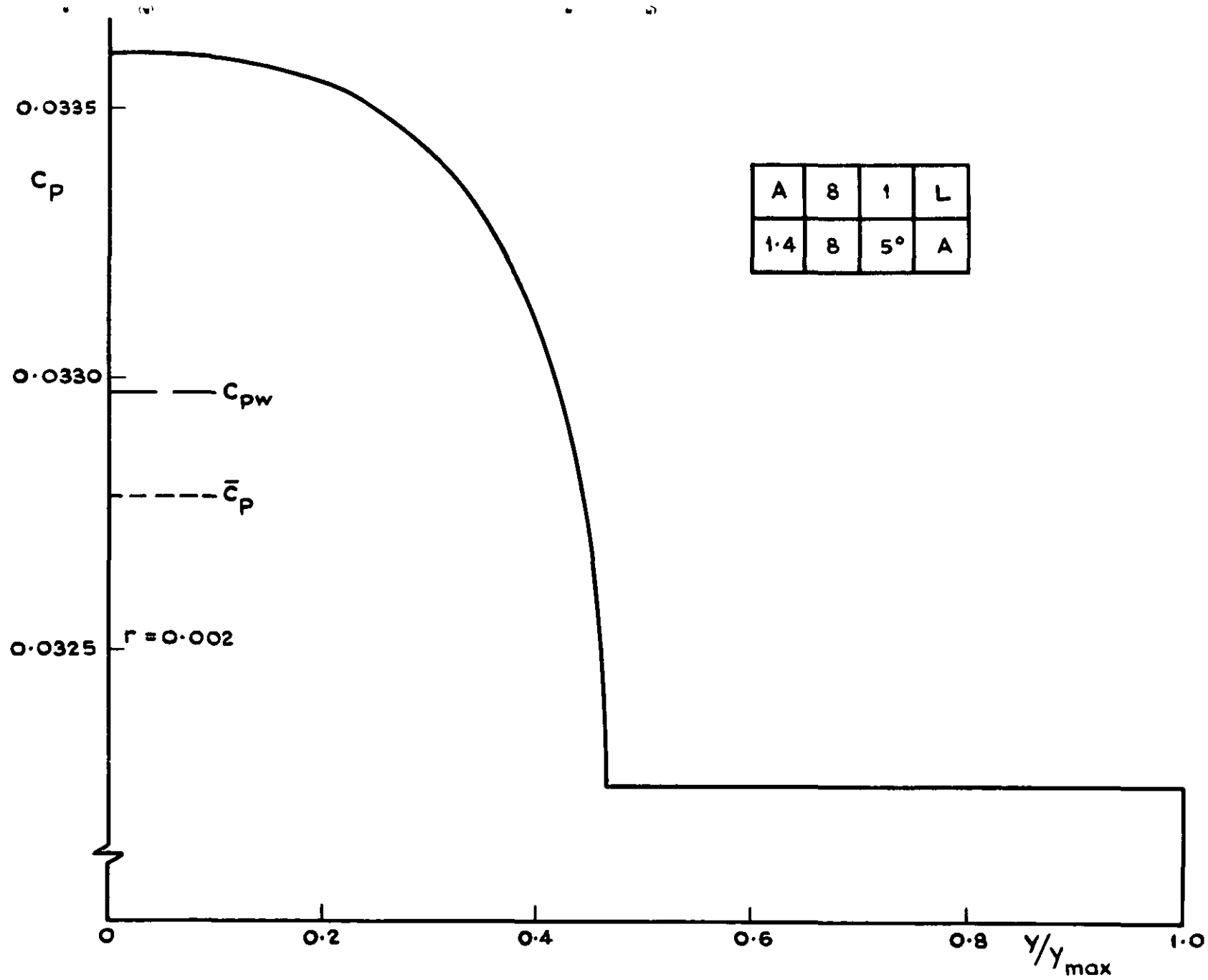


Fig.14 Wing A: Pressure distribution across span $M=8$, $\gamma=1.4$, $\alpha=5^\circ$

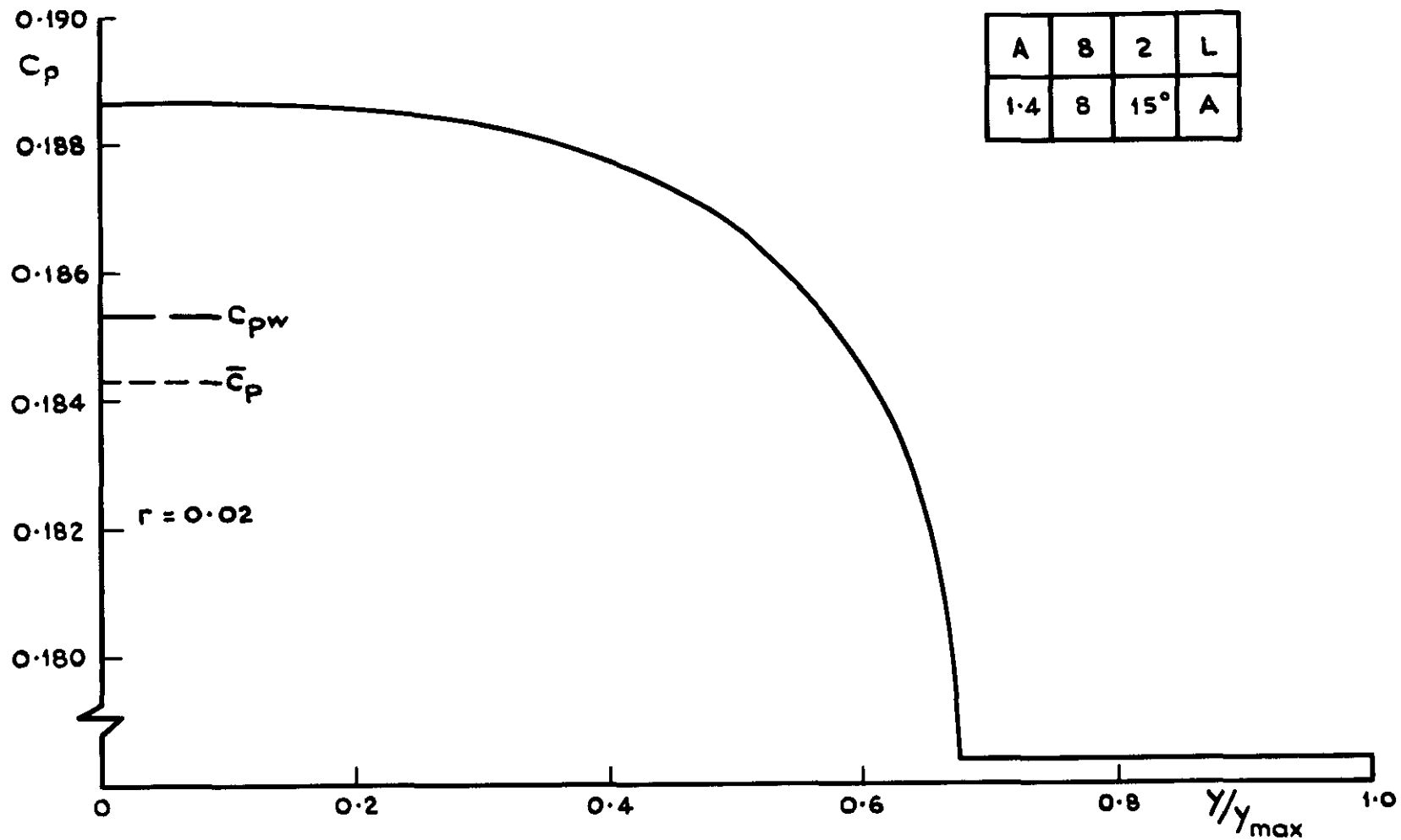


Fig.15 Wing A: Pressure distribution across span $M=8$, $\delta = 1.4$, $\alpha = 15^\circ$

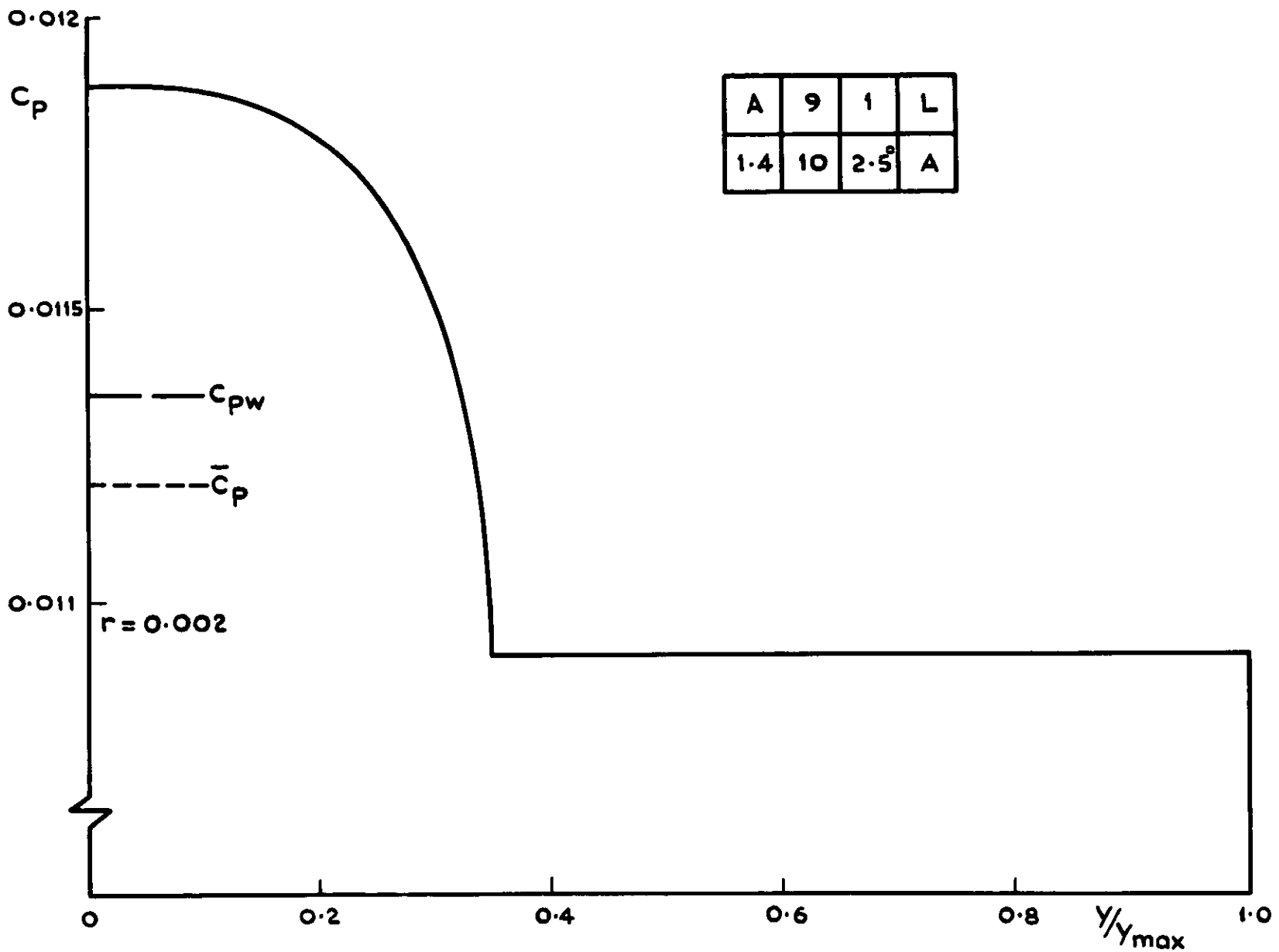


Fig.16 Wing A: Pressure distribution lower surface $M=10$, $\gamma = 1.4$, $\alpha = 2.5^\circ$

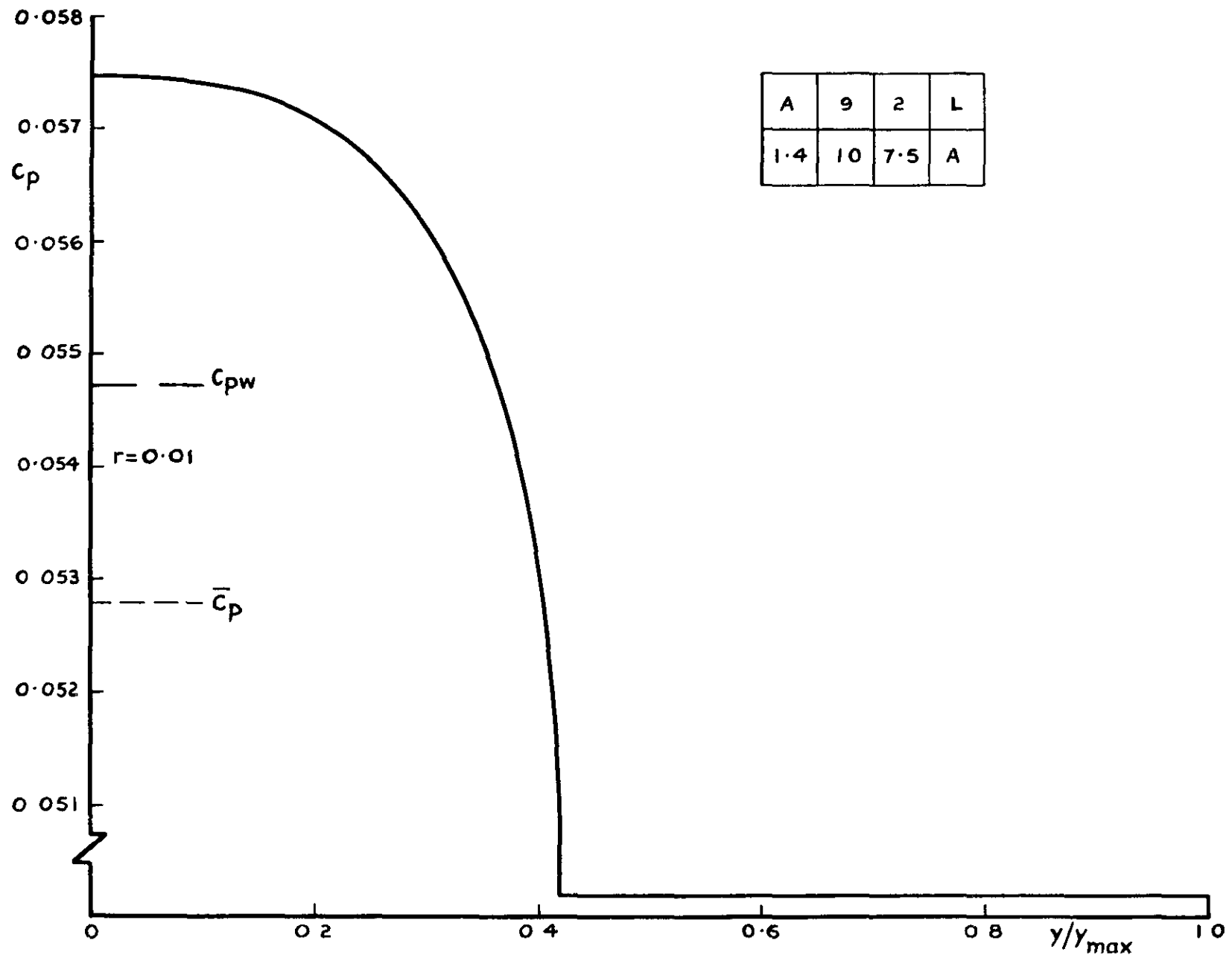


Fig.17 Wing A: Pressure distribution upper surface $M=10$, $\gamma=1.4$, $\alpha=7.5$

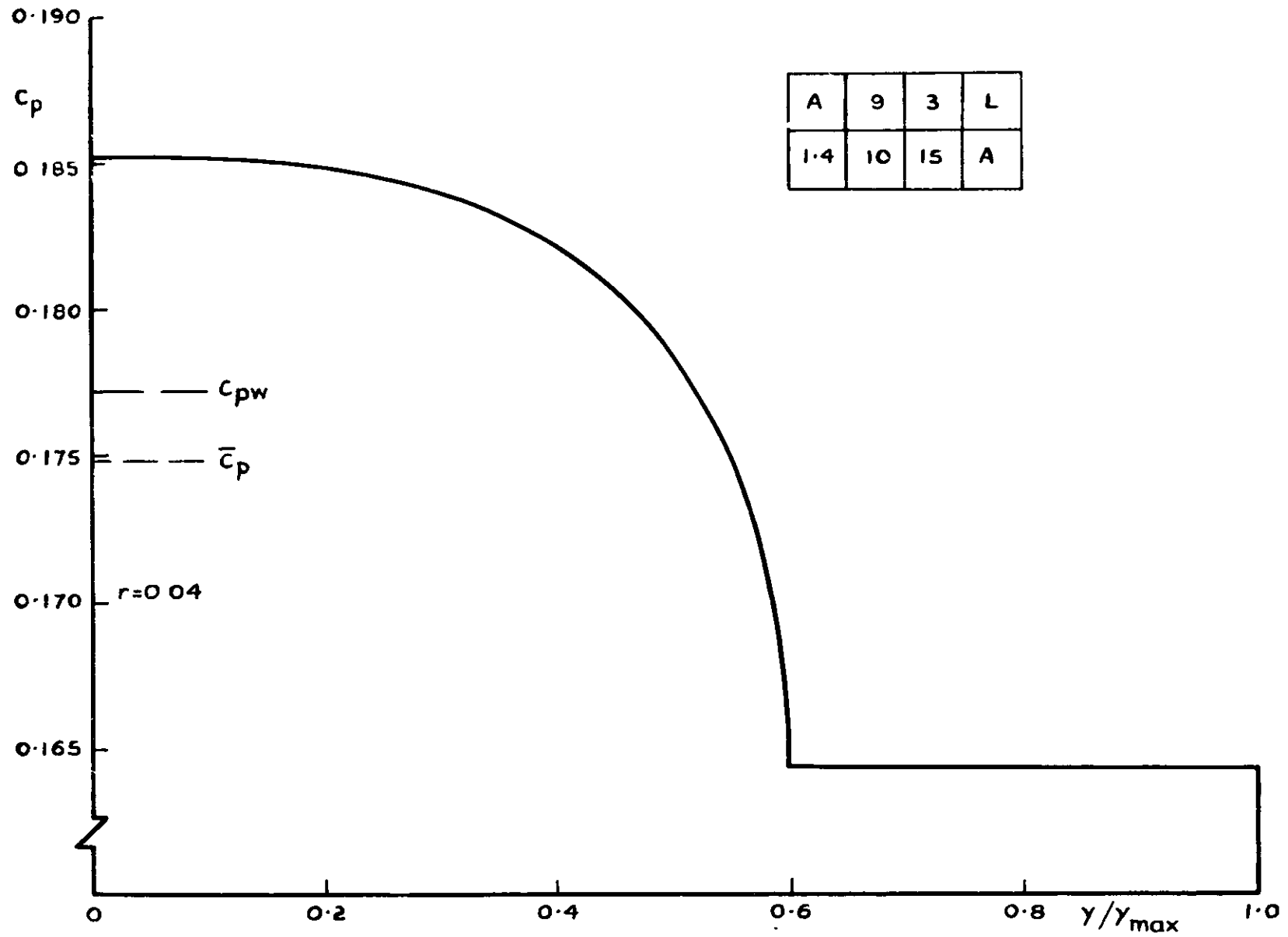


Fig.18 Wing A: Pressure distribution lower surface $M=10$, $\delta=1.4$, $\alpha=15^\circ$

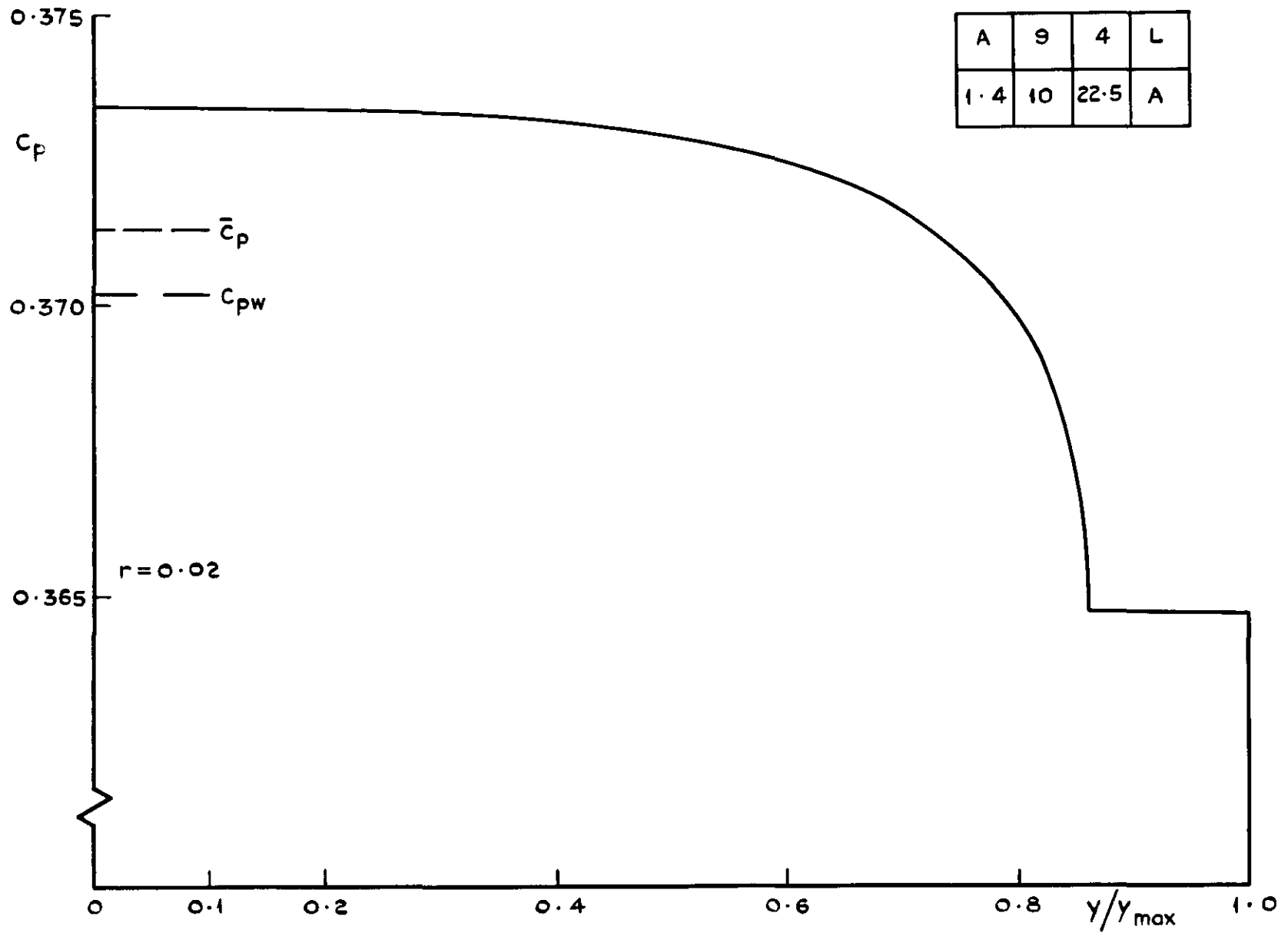


Fig.19 Wing A: Pressure distribution upper surface $M=10$, $\delta = 1.4$, $\alpha = 22.5$

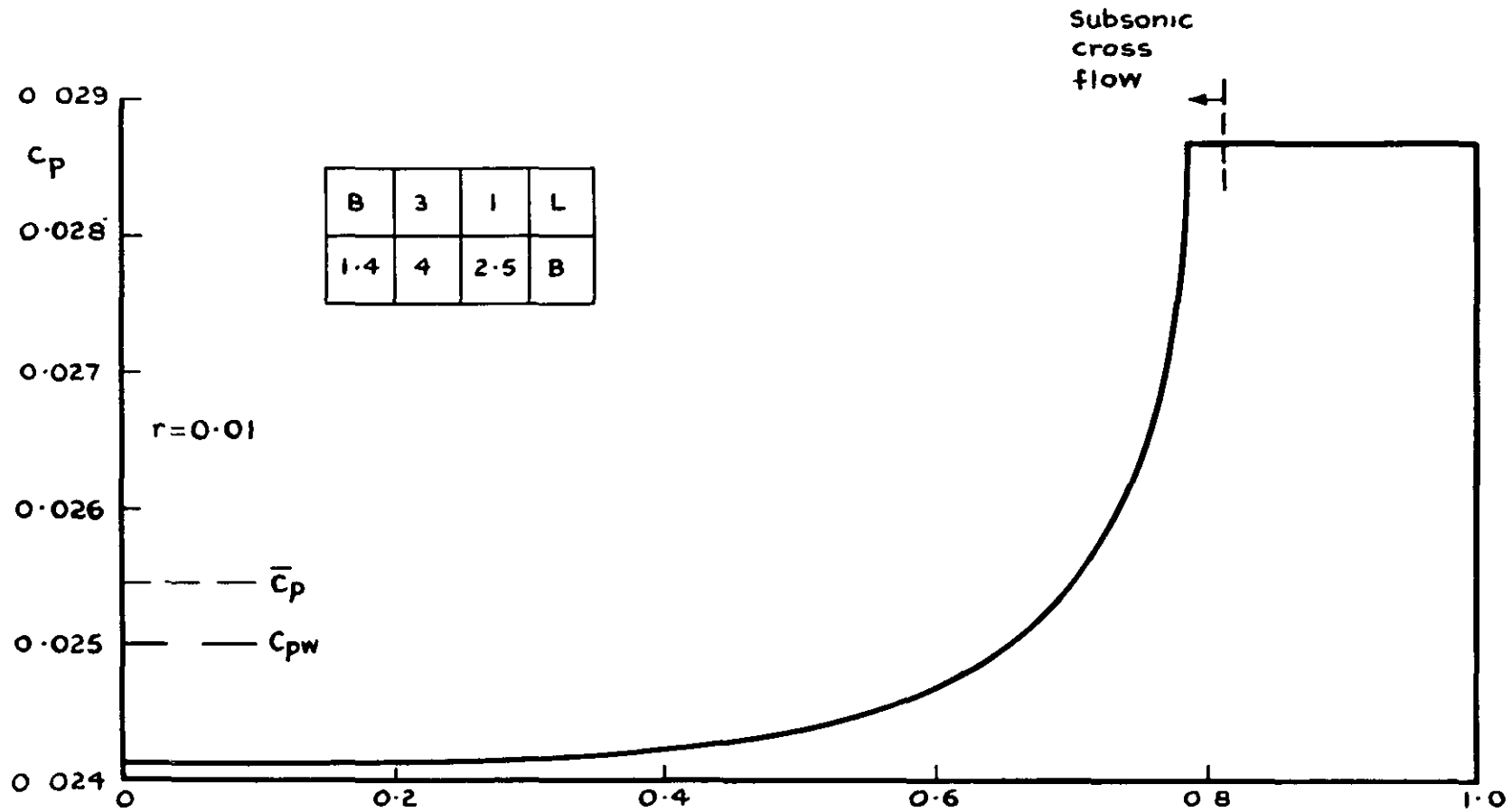


Fig.20 Wing B: Pressure distribution lower surface $M=4$, $\delta=1.4$, $\alpha=2.5^\circ$

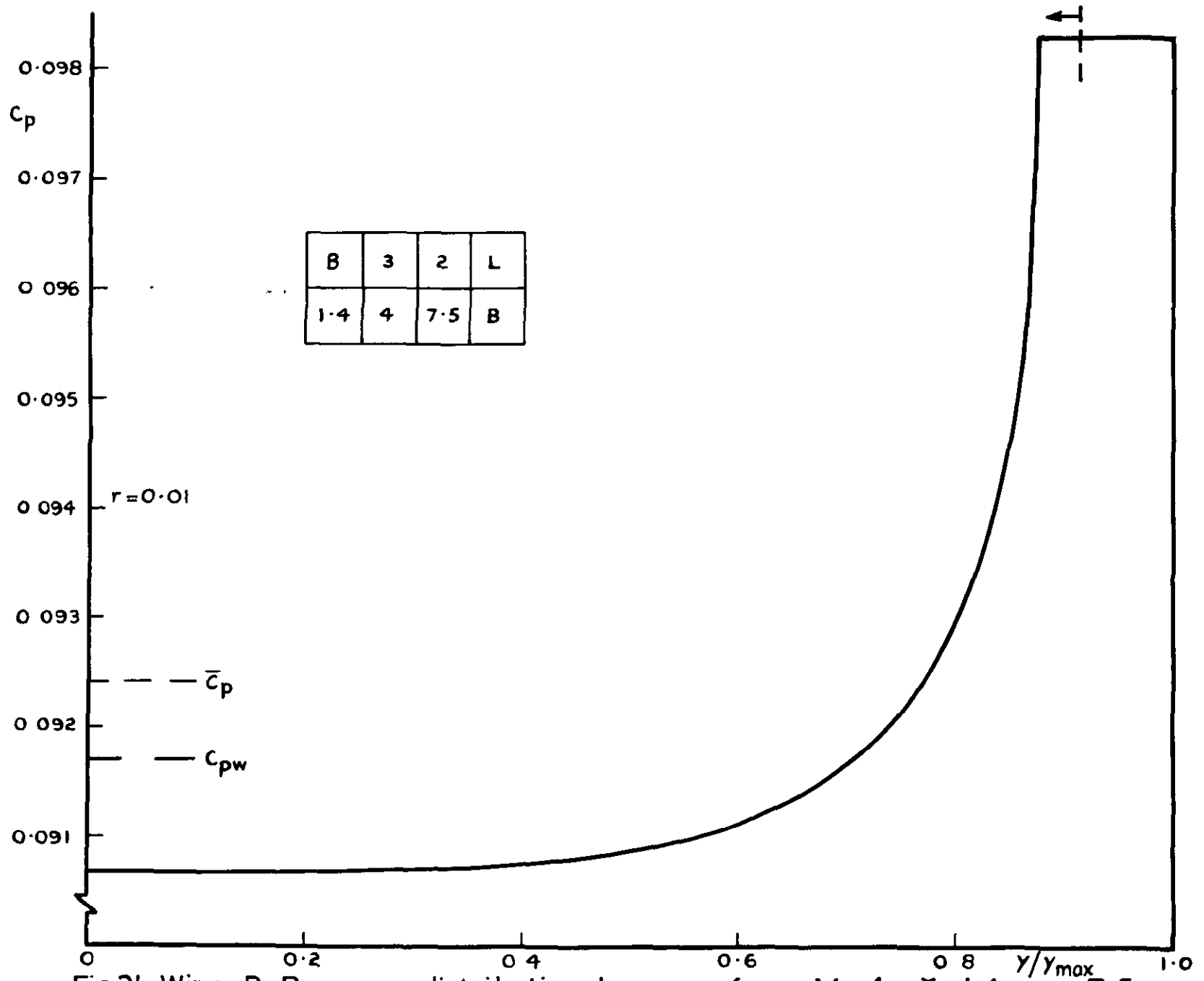


Fig 21 Wing B: Pressure distribution lower surface $M=4$, $\delta=1.4$, $\alpha=7.5$

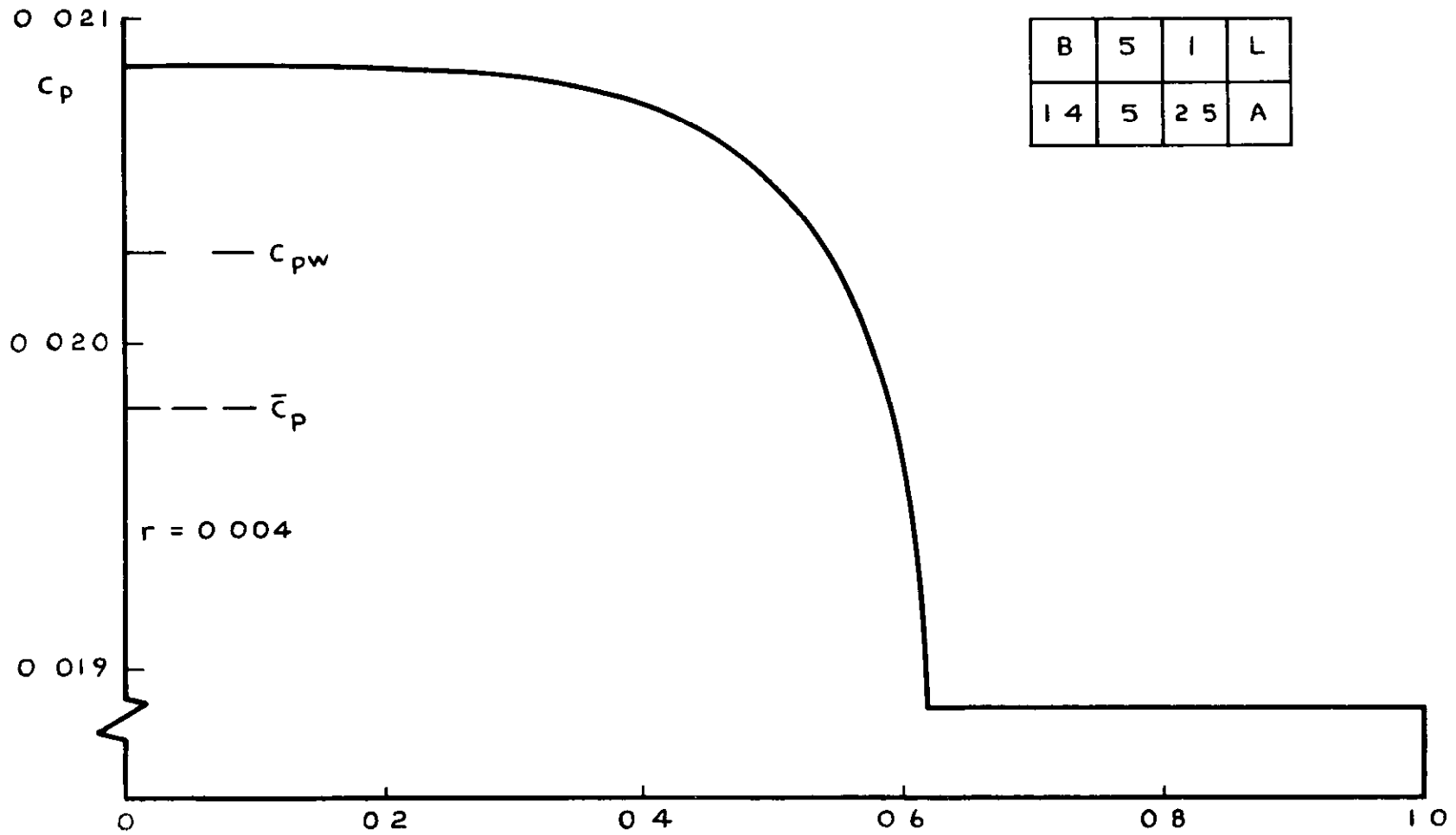


Fig. 22 Wing B: Pressure distribution lower surface $M = 5$, $\delta = 1.4$, $\alpha = 2.5^\circ$

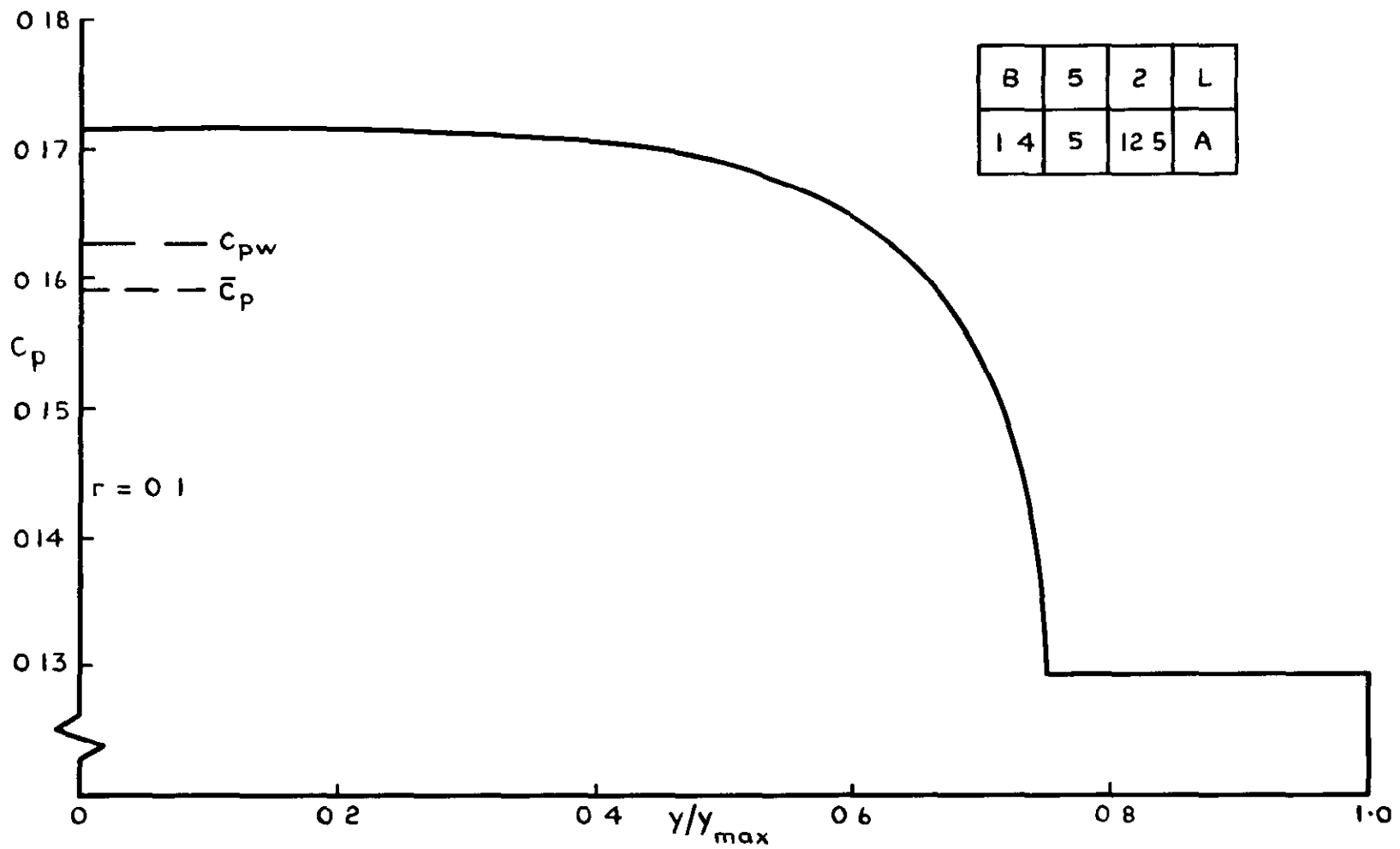


Fig 23 Wing B: Pressure distribution lower surface $M = 5$, $\delta = 1.4$, $\alpha = 12.5^\circ$

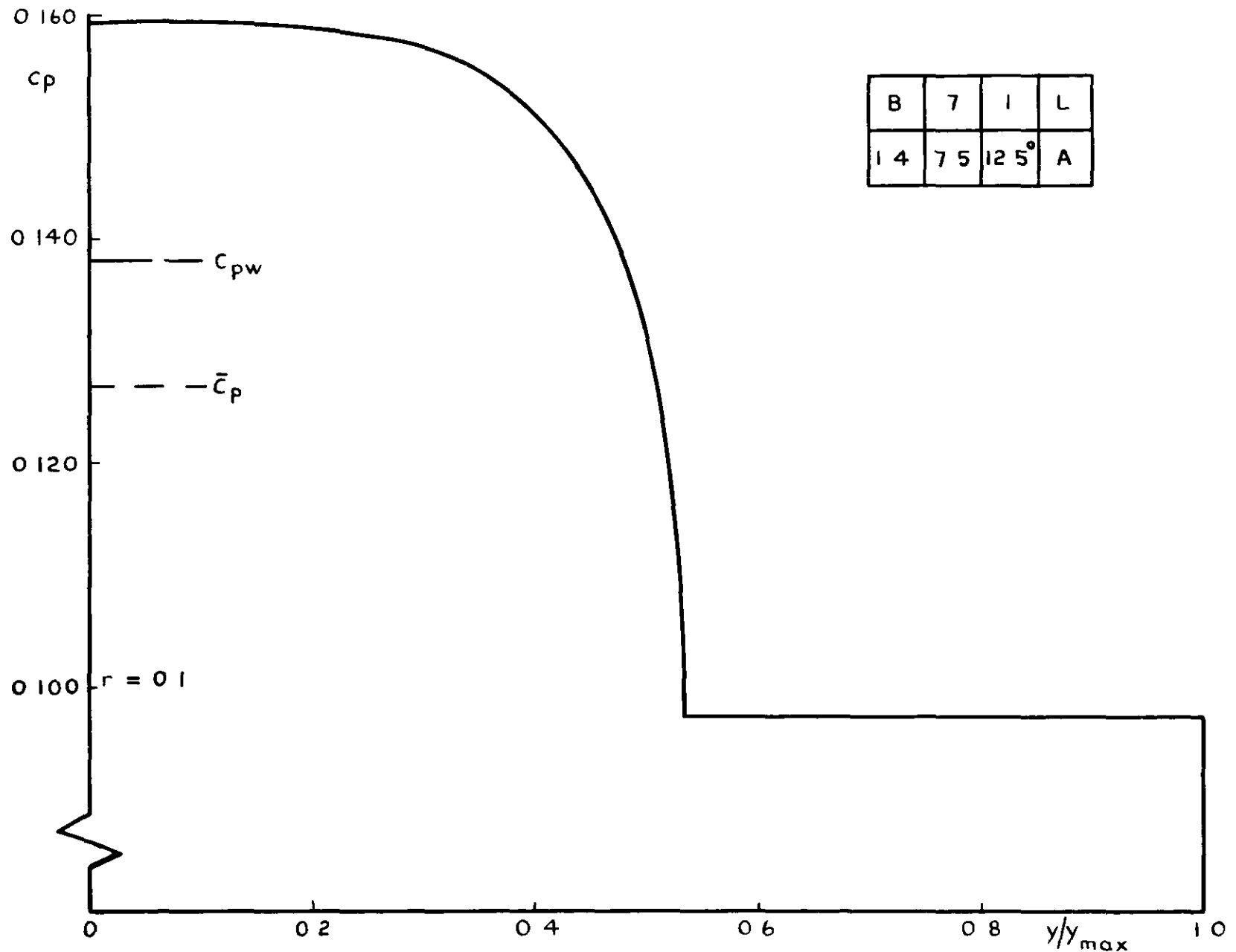


Fig. 24 Wing B. Pressure distribution lower surface $M = 7.5$, $\delta = 1.4$, $\alpha = 12.5^\circ$

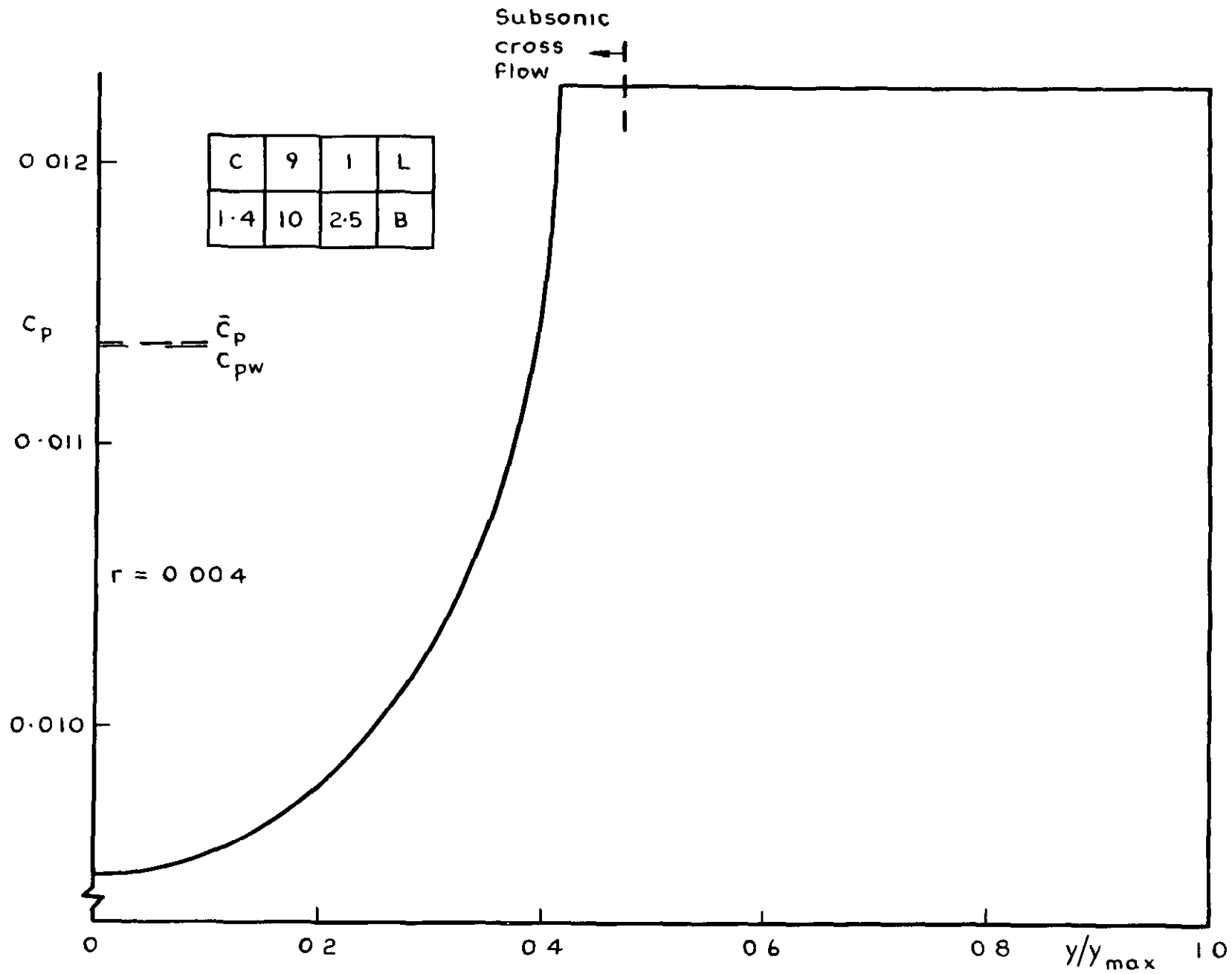


Fig. 25 Wing C: Pressure distribution lower surface $M = 10$, $\delta = 1.4$, $\alpha = 2.5^\circ$

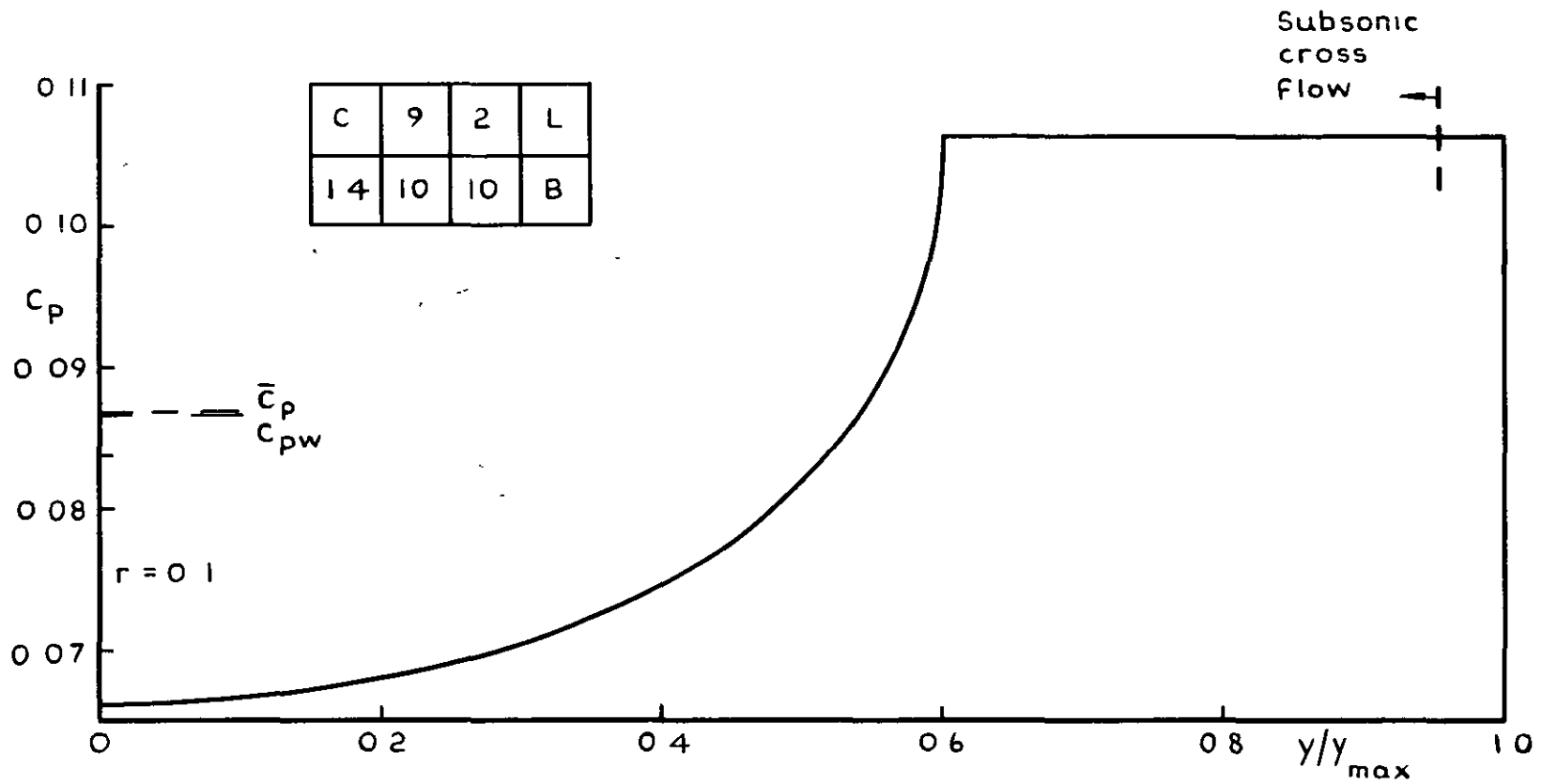


Fig. 26 Wing C: Pressure distribution lower surface $M = 10$, $\delta = 1.4$, $\alpha = 10^\circ$,

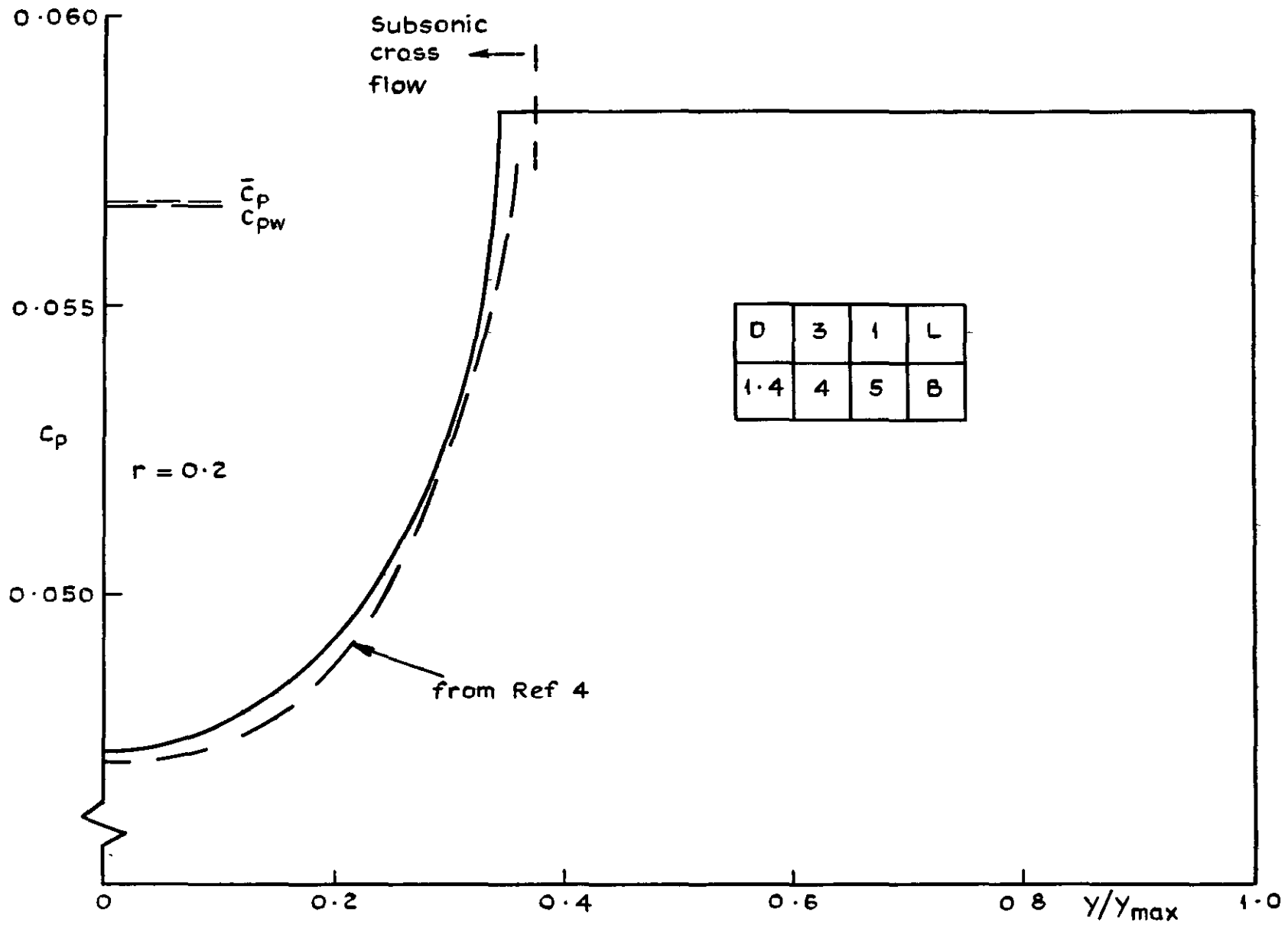


Fig.27 Wing D: Pressure distribution lower surface $M = 4$, $\delta = 1.4$, $\alpha = 5^\circ$

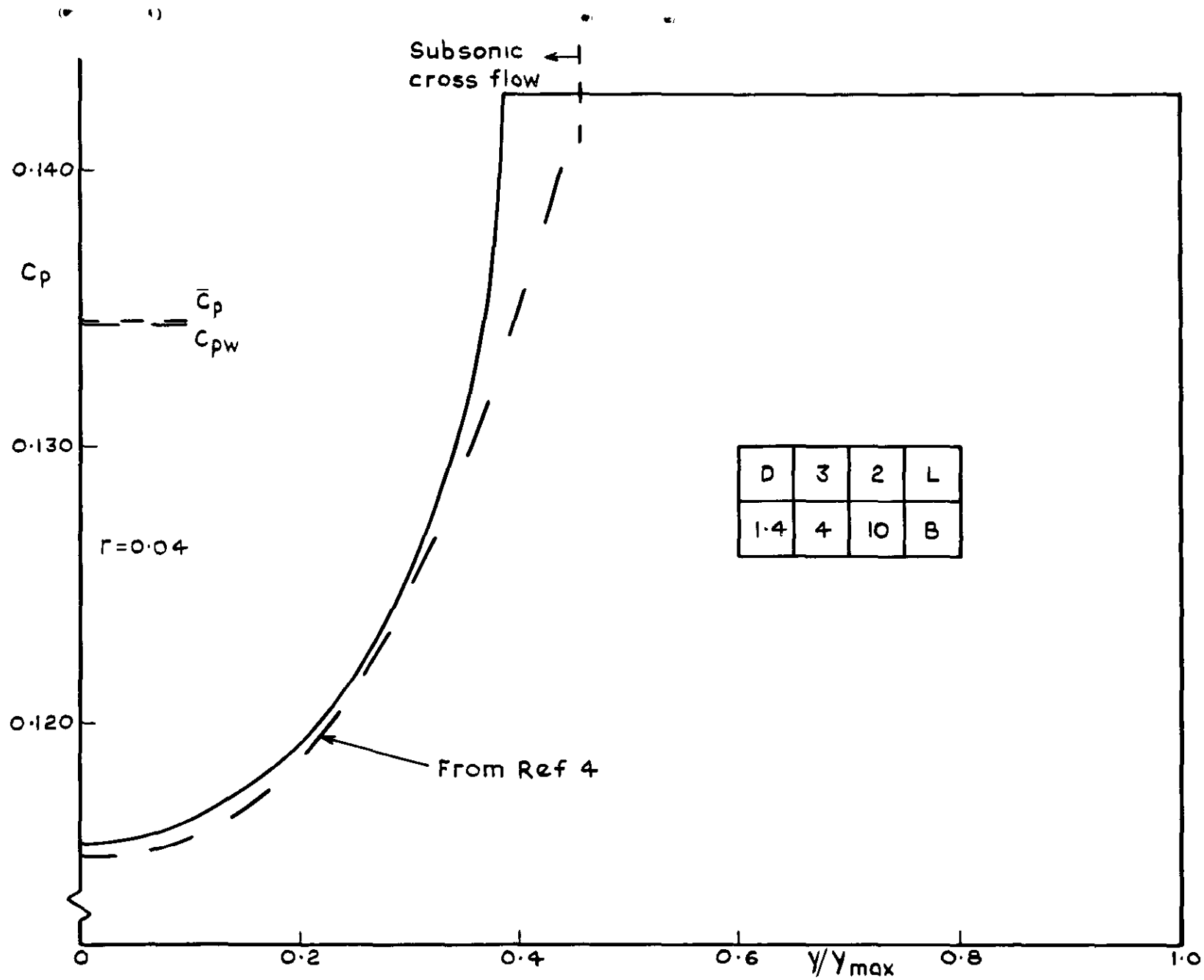


Fig 28 Wing D: Pressure distribution lower surface $M = 4$, $\delta = 1.4$, $\alpha = 10^\circ$

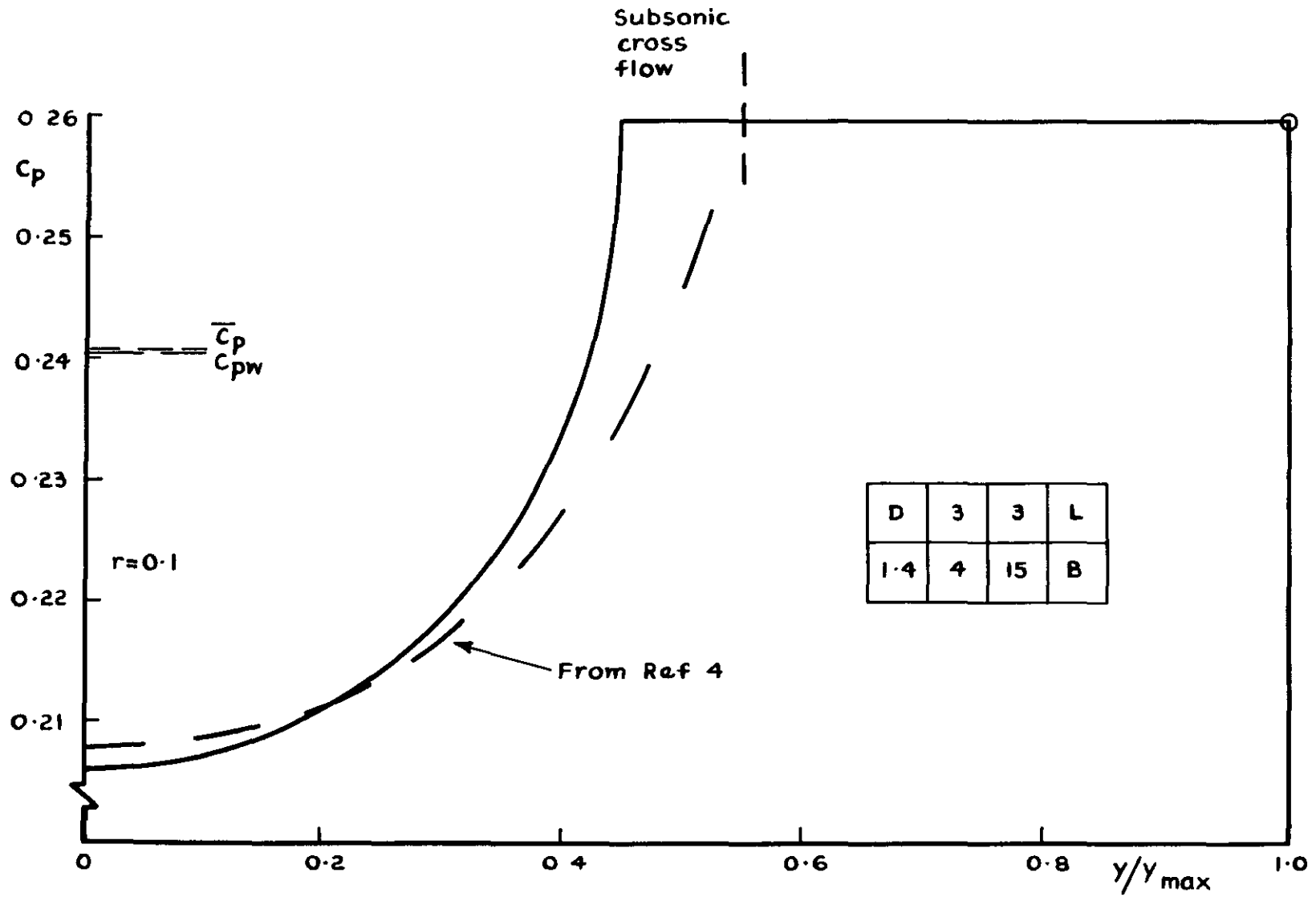


Fig.29 Wing D: Pressure distribution lower surface $M=4$, $\delta=1.4$, $\alpha=15^\circ$

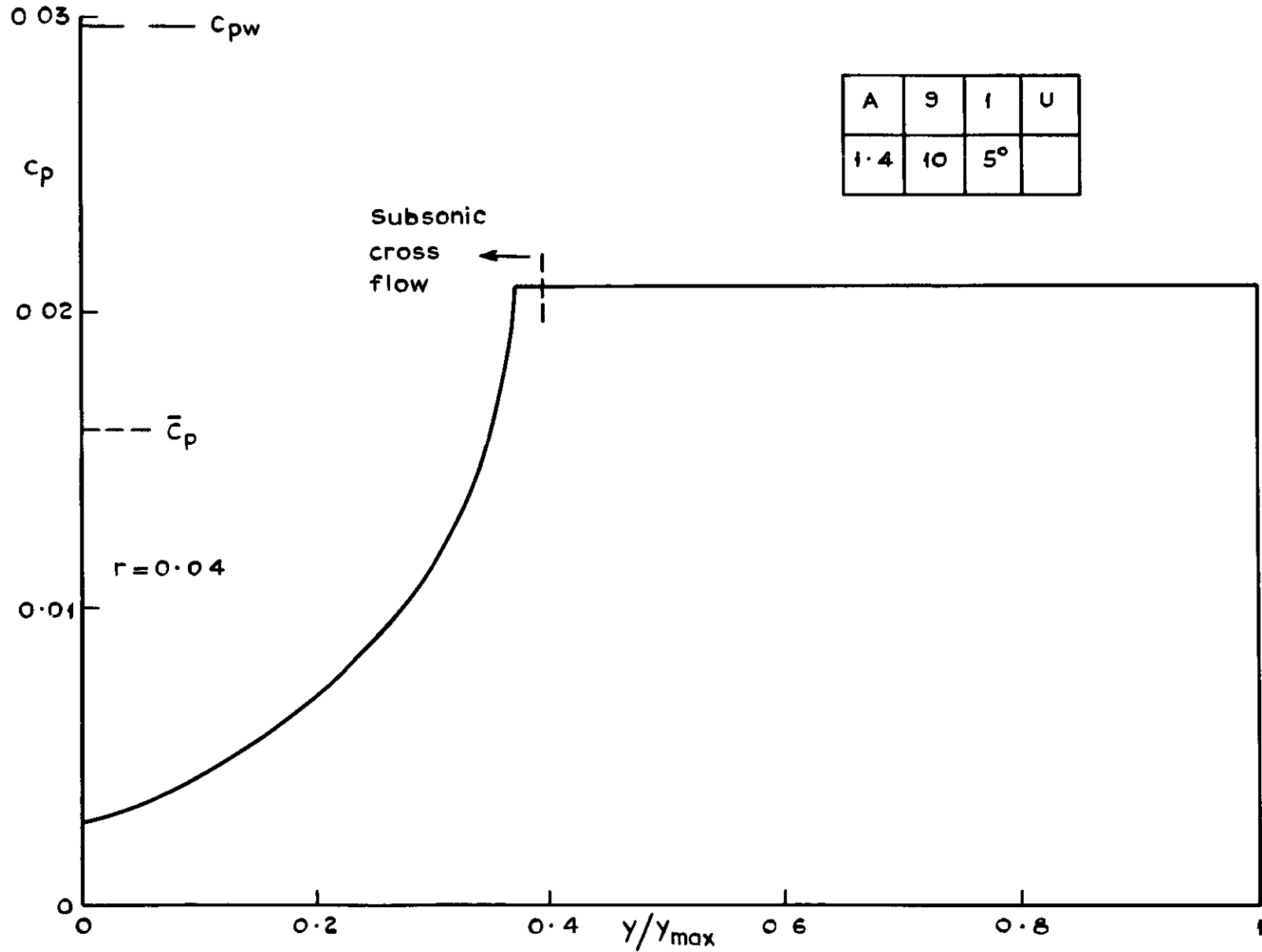


Fig.30 Wing A : Pressure distribution upper surface $M=10, \delta = 1.4, \alpha = +5^\circ$

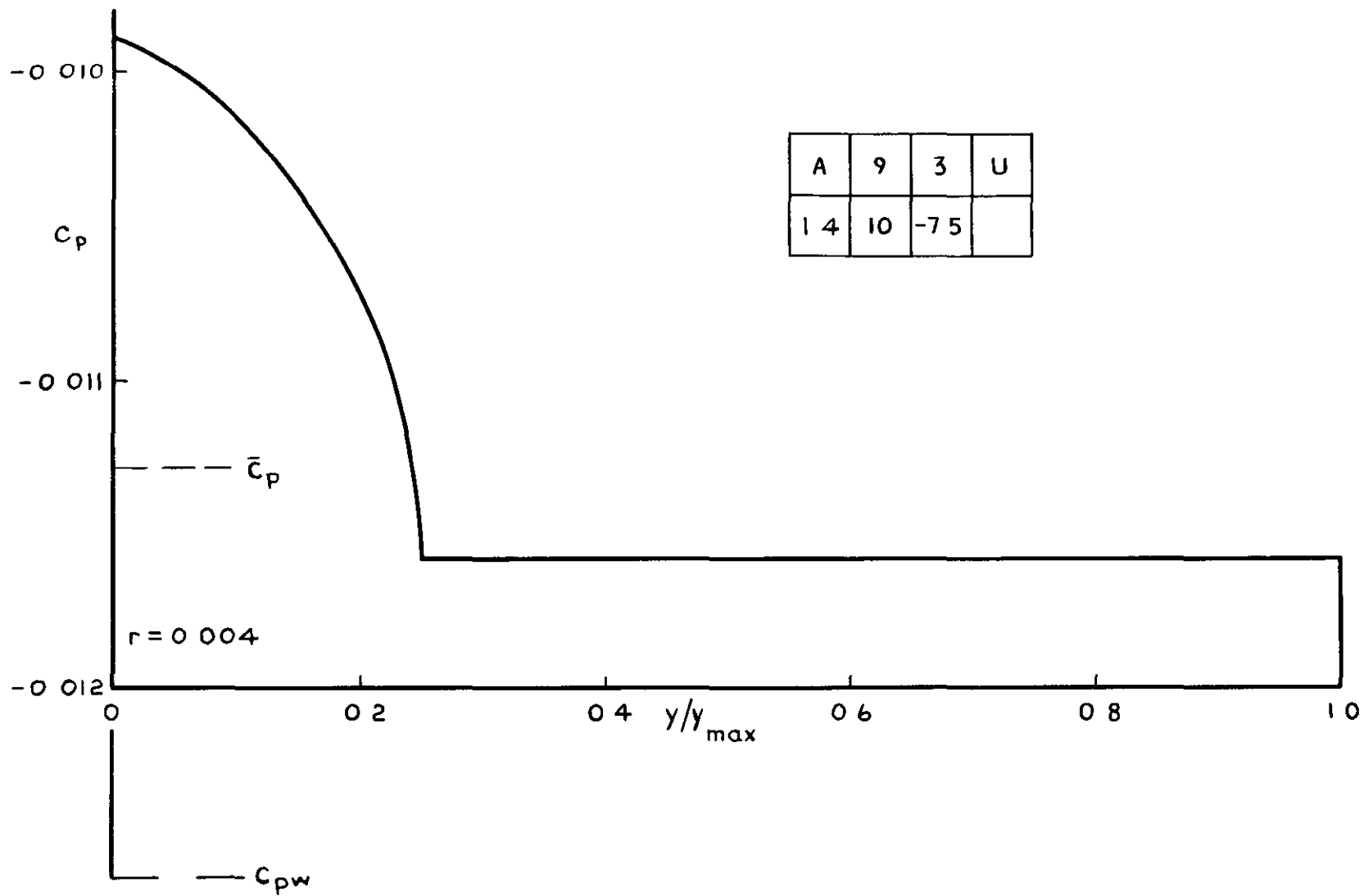


Fig. 31 Wing A: Pressure distribution upper surface $M = 10$, $\delta = 1.4$, $\alpha = -7.5^\circ$

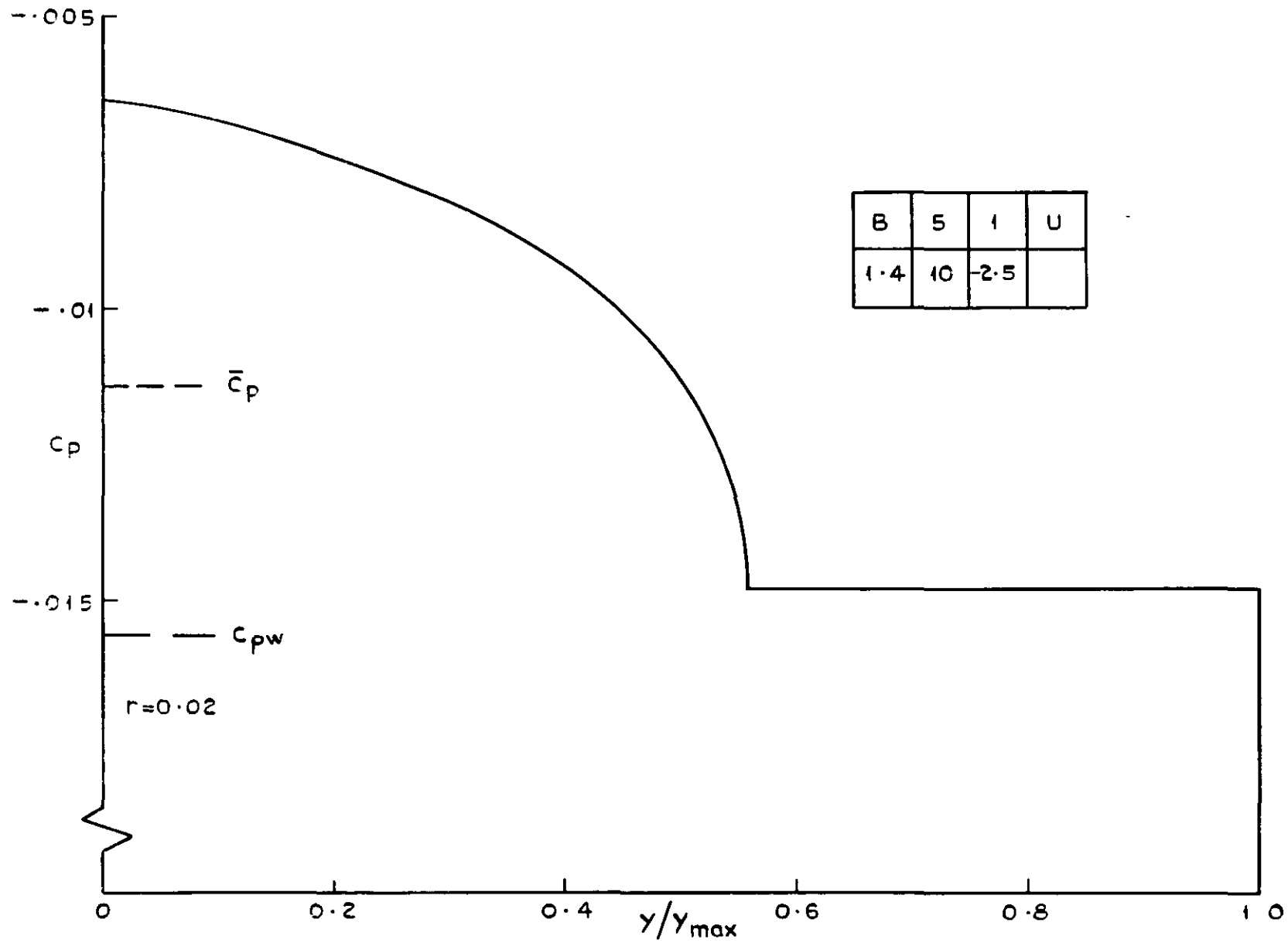


Fig.32 Wing B: Pressure distribution upper surface $M=5$, $\gamma=1.4$, $\alpha=-2.5^\circ$

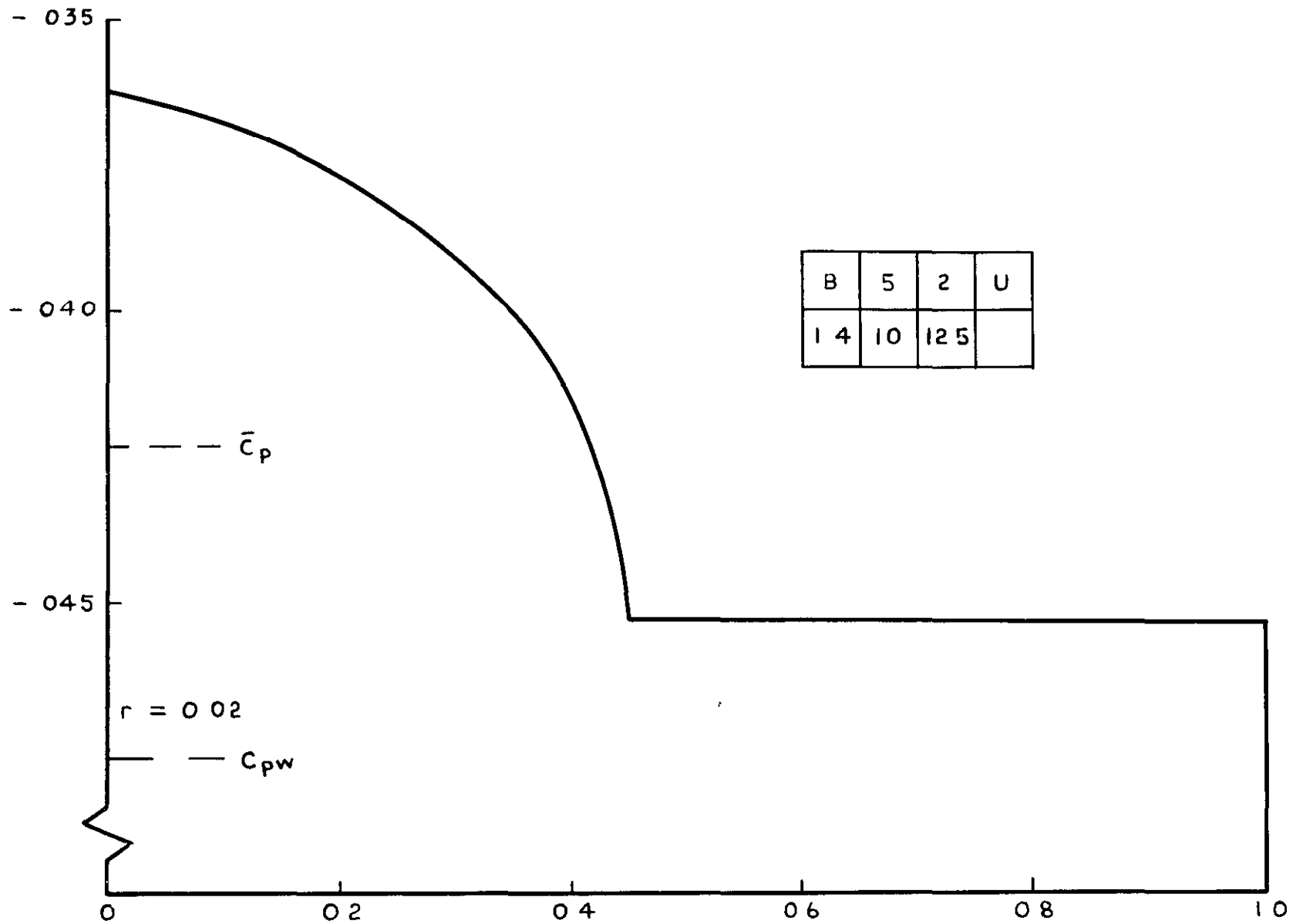


Fig. 33 Wing B: Pressure distribution upper surface $M = 5$, $\gamma = 1.4$, $\alpha = 12.5^\circ$

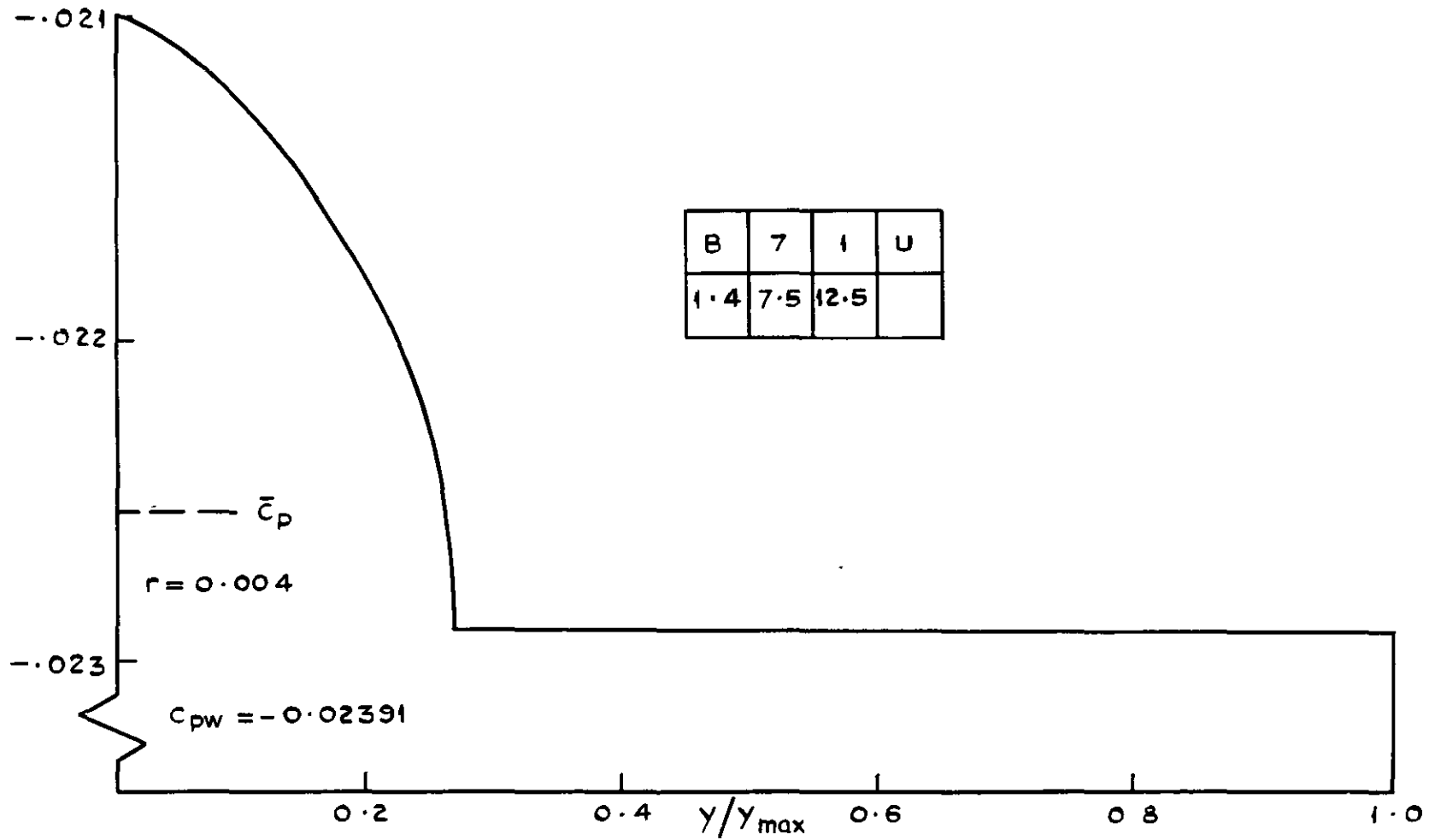


Fig.34 Wing B : Pressure distribution upper surface $M = 7.5, \delta = 1.4, \alpha = 12.5^\circ$

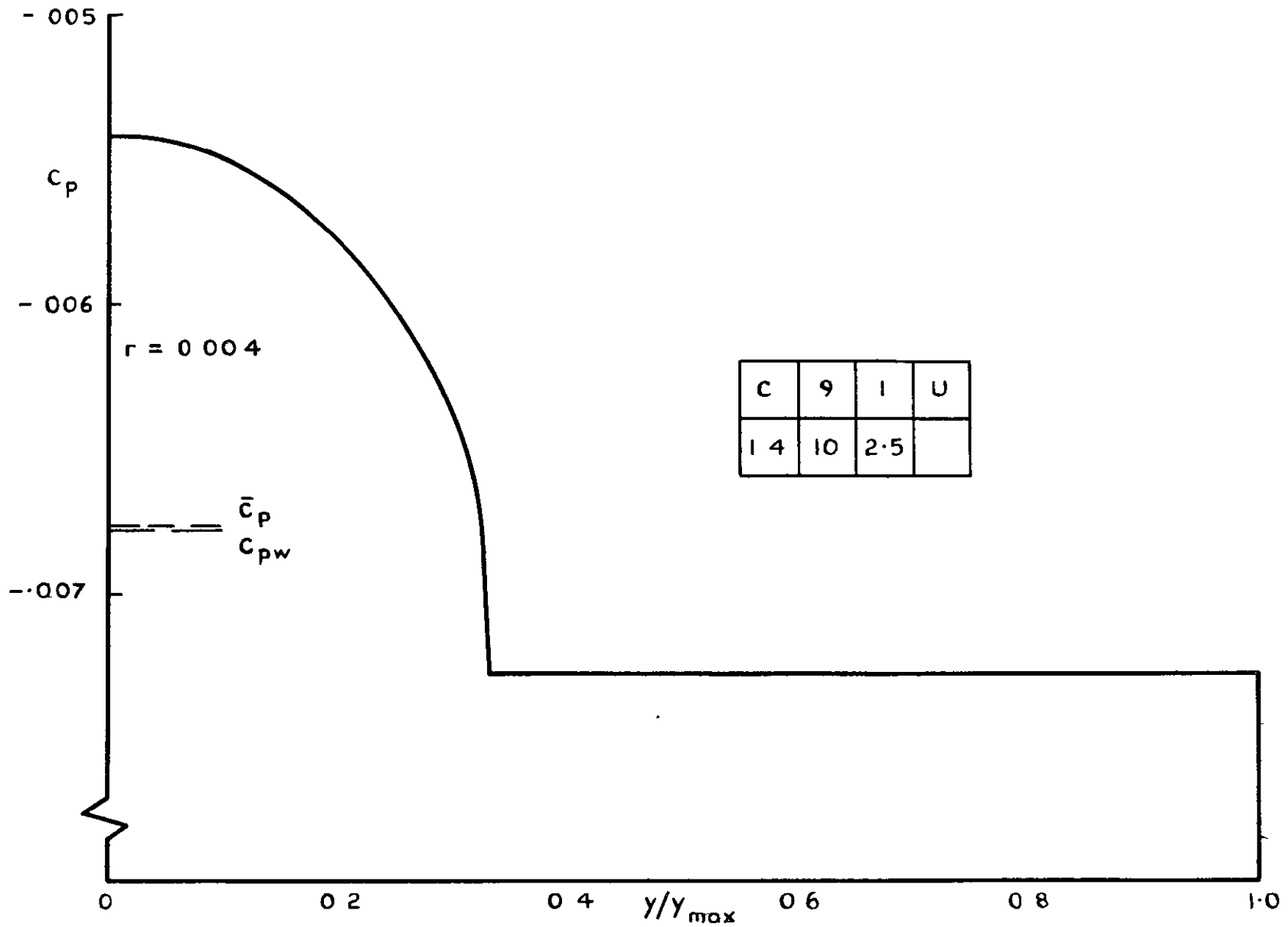


Fig. 35 Wing C: Pressure distribution upper surface $M = 10, \gamma = 1.4, \alpha = 2.5^\circ$

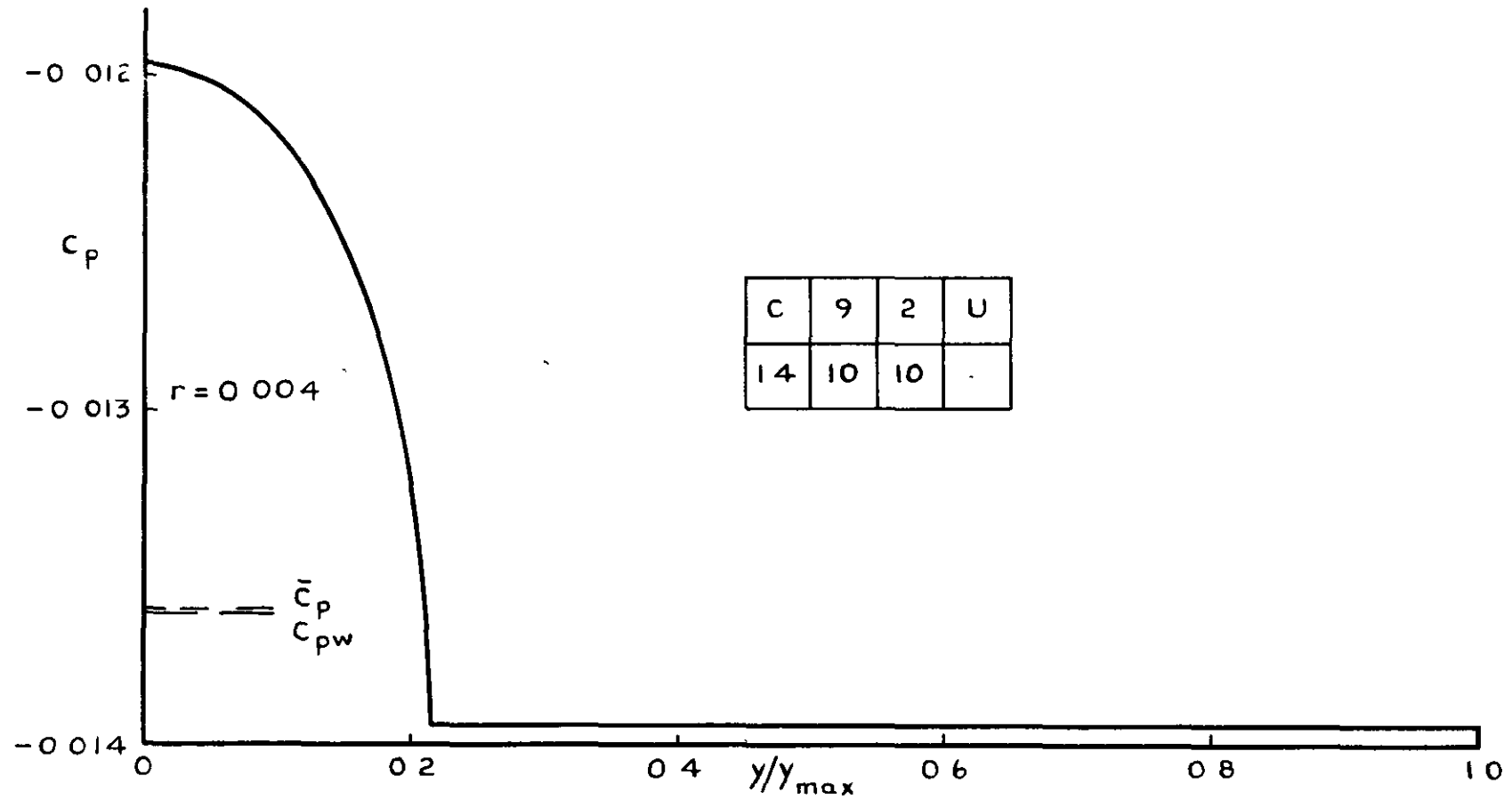


Fig 36 Wing C. Pressure distribution upper surface $M = 10$, $\delta = 1.4$, $\alpha = 10^\circ$,

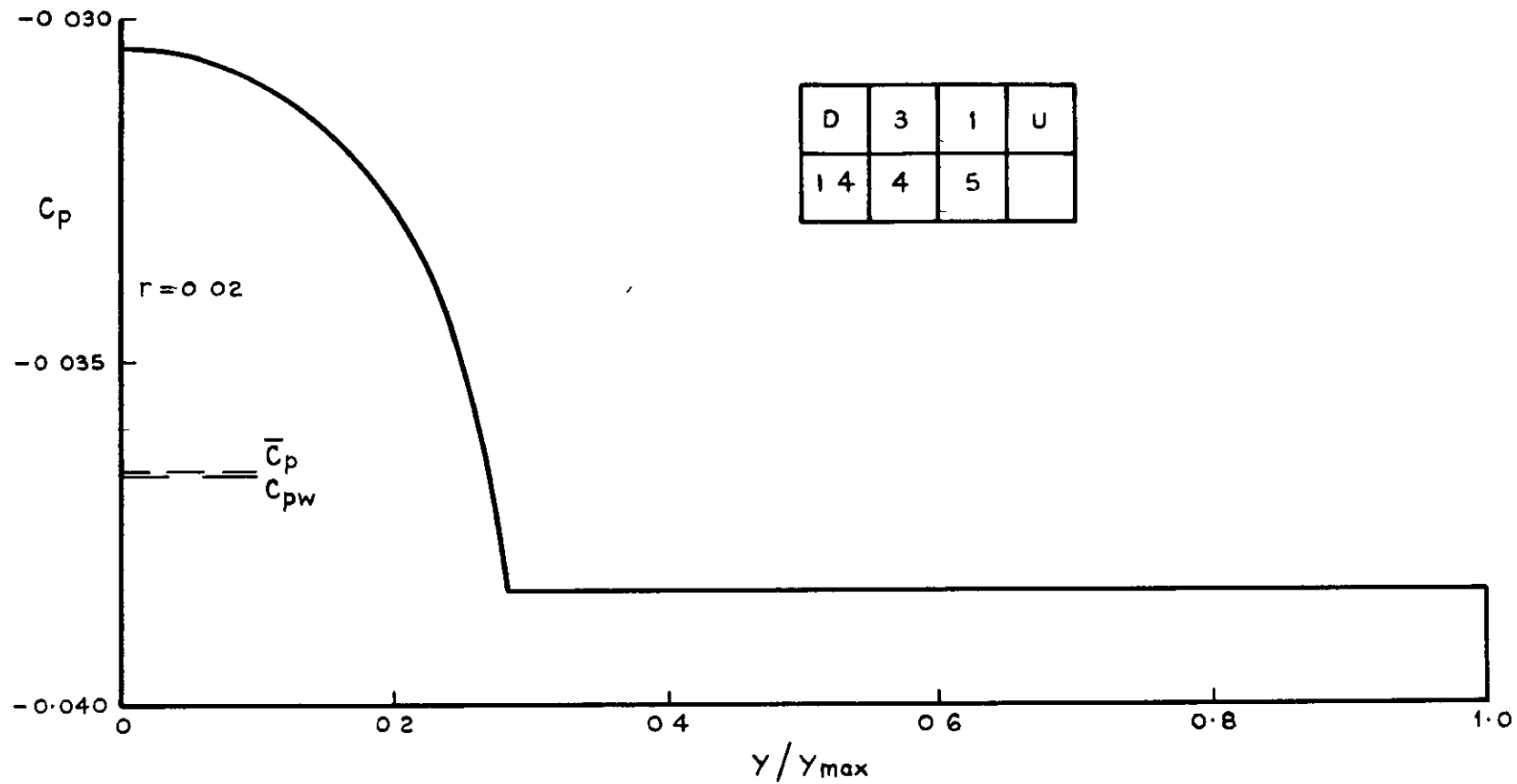


Fig. 37 Wing D: Pressure distribution upper surface $M = 4$, $\tau = 1.4$, $\alpha = 5^\circ$

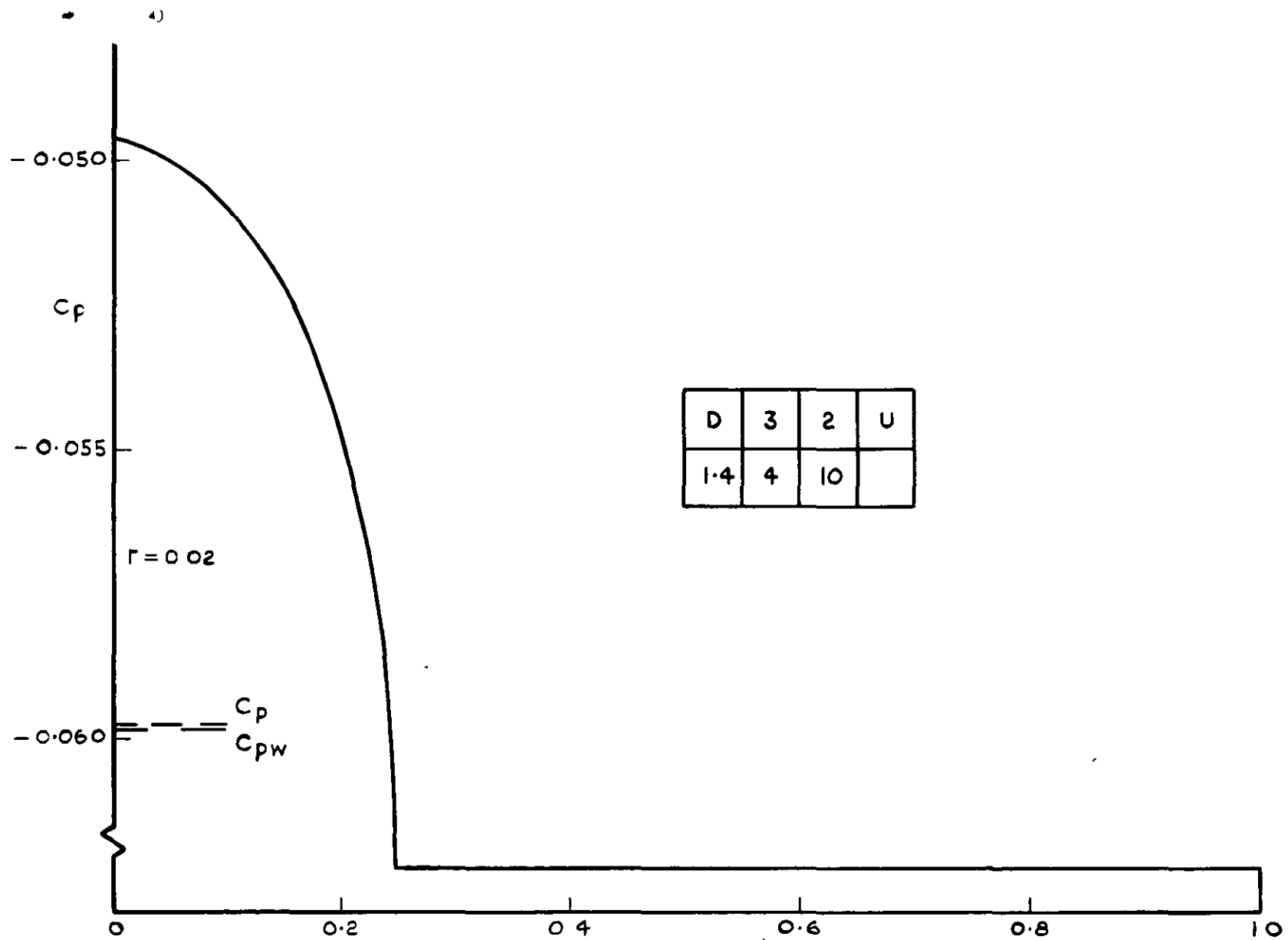


Fig 38 Wing D: Pressure distribution upper surface $M = 4$, $\gamma = 1.4$, $\alpha = 10^\circ$

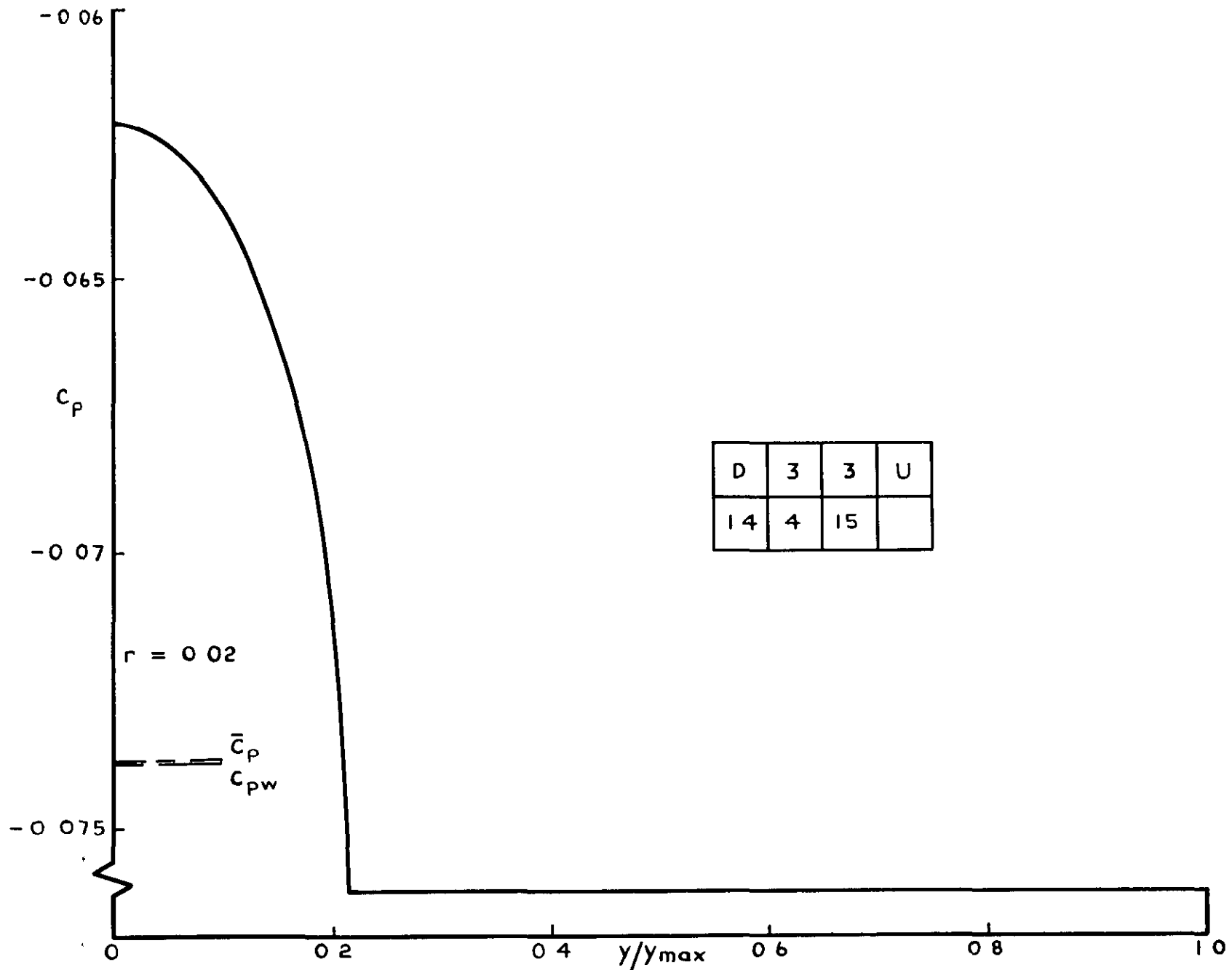


Fig. 39 Wing D: Pressure distribution upper surface $M = 4$, $\delta = 1.4$, $\alpha = 15^\circ$

DETACHABLE ABSTRACT CARD

A.R.C. C.P. No.1178
March 1971

Pike, J.

THEORETICAL PRESSURE DISTRIBUTIONS ON
FOUR SIMPLE WING SHAPES FOR A RANGE OF
SUPERSONIC FLOW CONDITIONS

Pressure distributions are presented for four conical wing shapes with attached shock waves at their leading edges. The wings are those proposed after Euromech 20 as reference shapes for the comparison of flow prediction methods. The influence on the pressure distribution of wing incidence, free stream Mach number or ratio of specific heats is demonstrated. Some pressure distributions over the upper surface are also presented, assuming an isentropic expansion at the leading edge.

533 692.55
533.693 3
533 6 048.2
533.6.011 72
533.6.011.5

Pressure distributions are presented for four conical wing shapes with attached shock waves at their leading edges. The wings are those proposed after Euromech 20 as reference shapes for the comparison of flow prediction methods. The influence on the pressure distribution of wing incidence, free stream Mach number or ratio of specific heats is demonstrated. Some pressure distributions over the upper surface are also presented, assuming an isentropic expansion at the leading edge.

THEORETICAL PRESSURE DISTRIBUTIONS ON
FOUR SIMPLE WING SHAPES FOR A RANGE OF
SUPERSONIC FLOW CONDITIONS

A.R.C. C.P. No.1178
March 1971
Pike, J.

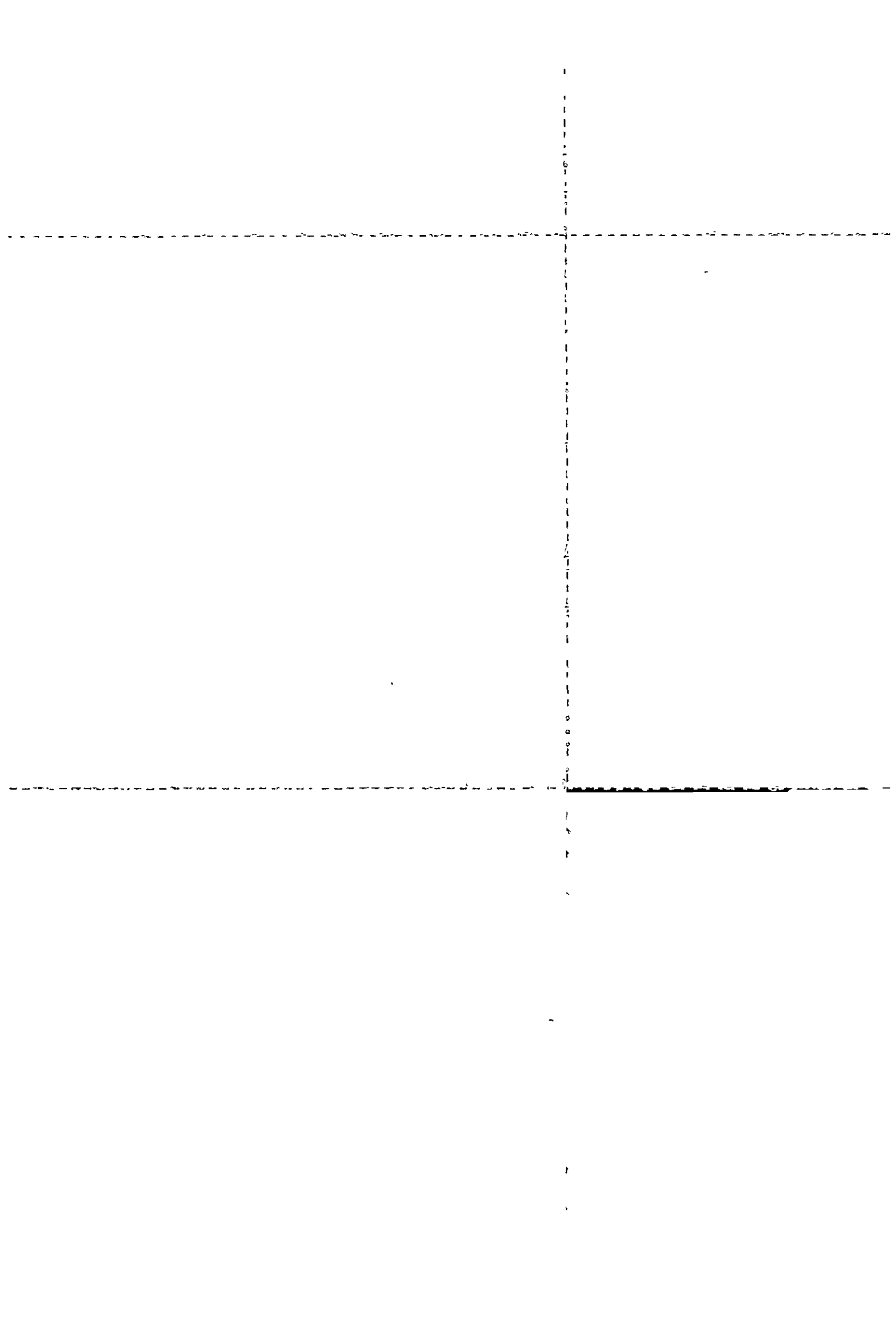
533.692.55
533 6.048.2
533.6.011 72
533.6 011.5

THEORETICAL PRESSURE DISTRIBUTIONS ON
FOUR SIMPLE WING SHAPES FOR A RANGE OF
SUPERSONIC FLOW CONDITIONS

A.R.C. C.P. No.1178
March 1971
Pike, J.

533.692.55
533 6.048.2
533.6.011.72
533.6.011.5

Pressure distributions are presented for four conical wing shapes with attached shock waves at their leading edges. The wings are those proposed after Euromech 20 as reference shapes for the comparison of flow prediction methods. The influence on the pressure distribution of wing incidence, free stream Mach number or ratio of specific heats is demonstrated. Some pressure distributions over the upper surface are also presented, assuming an isentropic expansion at the leading edge.



C.P. No. 1178

© *Crown copyright 1971*

Published by
HER MAJESTY'S STATIONERY OFFICE

To be purchased from
49 High Holborn, London WC1 V 6HB
13a Castle Street, Edinburgh EH2 3AR
109 St Mary Street, Cardiff CF1 1JW
Brazenose Street, Manchester M60 8AS
50 Fairfax Street, Bristol BS1 3DE
258 Broad Street, Birmingham B1 2HE
80 Chichester Street, Belfast BT1 4JY
or through booksellers

C.P. No. 1178

SBN 11 470446 5